On the Calibration of the SABR Model and its Extensions

by

Cheng Luo (CID: 01153695)

Department of Mathematics
Imperial College London
London SW7 2AZ
United Kingdom

Thesis submitted as part of the requirements for the award of the MSc in Mathematics and Finance, Imperial College London, 2015-2016

The work contained in this thesis is my own work unless otherwise stated.

Signed: Date:

I would first like to thank my thesis supervisor Dr. Thomas Cass at Imperial College London who consistently gave me help and encouragement whenever he thought I needed it.

I would also like to thank Mr. Matthew Brown, at Citadel LLC, for providing me insights on relevant technical subjects.

Finally, I must express my very profound gratitude to my parents for providing me with unfailing support and continuous encouragement throughout my years of study.

Contents

1 Introduction

The Libor market model (LMM) seems to be the most promising model family among the interest rate models [9]. Unlike the short rate models, it is able to capture the dynamics of the entire curve of interest rates by using Libor forwards as its ingredients. However, a drawback of the LMM model is that it is less flexible in modelling the essential characteristics of interest rate markets, in particular, the volatility smile.

The Stochastic Alpha, Beta, Rho (SABR) model attempts to address this unsolved issue in the classic LMM model by assuming the volatility itself as a stochastic process. The model has been widely applied over the years since Hagan and his co-workers derived the analytical approximation of the Black implied volatility [12]. It has gained its attention in the finance world due to the simplicity of the model dynamics and the ability of fitting the subtle differences in the shape of the implied volatility smile. A large number of studies on the SABR model extensions has also been conducted to cope with different practical issues raised in the use of the model. In particular, the λ-SABR model, which is the classic SABR model with a mean-reversion term seems to produce a better approximation of the Black Scholes implied volatility [1]. In the latter paper, Labordère derived the analytic approximation formula using the heat kernel expansion on a Riemannian manifold. Several alternative methods were used in the literature to obtain such approximations: singular perturbation analysis, Malliavin calculus [18] [6], and transition density [19].

Rebonato proposed the SABR extension on the Libor market model in order to take advantage on the SABR model's ability of fitting volatility smile [2] [11].

In this thesis, we aim to study the SABR model and its extension by carrying out theoretical and empirical analysis. In the first part of the thesis, we conduct a brief introduction to the basics of vanilla interest rate derivatives pricing for not familiar readers. The second part will devote to the literature review on the theory and application of the mentioned models. Then, we shall put the theories into practice to actually implement and calibrate the models with market data. Finally, we draw conclusions according to our empirical analysis and results.

2 Basic Concept

In this section, we briefly describe the instruments involved in this thesis. Some of the basic fixed income derivatives such as interest rate swap, cap/floor, and swaption will be presented. Term structures, valuation formulae and market practice on cap/floor and swaption pricing are introduced to readers who are not familiar with the subject.

2.1 Interest Rate Swap

Swap is an over-the-counter agreement between two counter-parties to exchange cash flows in the future. It is a very common and frequently traded fixed income derivative usually used to transform a liability or an asset. Many financial institutions also perform market making on swaps. In this thesis, we are interested in interest rate swap (IRS) and its valuation.

By signing a IRS contract, the issuer company agrees to pay a predetermined fixed rate on the notional [1] amount for a predetermined time range in exchange of payments at a floating rate on the same amount at the same time from receiver company. The floating rate agreed inter-bank is typically the Libor rate. The discounted pay-off of an issuer IRS is:

$$\begin{aligned} \mathrm{PV_{IRS}(t)} &= \sum_{i=\alpha+1}^{\beta} D(t,T_i)\tau_i(L(T_{i-1},T_i)-K) \qquad (2.1)\\ &= D(t,T_\alpha)\sum_{i=\alpha+1}^{\beta} D(T_\alpha,T_i)\tau_i(L(T_{i-1},T_i)-K). \qquad (2.2)\end{aligned}$$

In the above IRS, the issuer pays fixed rate K, receives Libor rate. $D(t,T_i)$ is the discount factor, $L(T_{i-1},T_i)$ is the Libor rate reset at T_{i-1} paid at T_i, and $\tau_i = T_i - T_{i-1}$ is the year fraction. The agreement is reset at $T_\alpha, T_{\alpha+1}, \cdots, T_{\beta-1}$ the payments are made at $T_\alpha + 1, T_{\alpha+2}, \cdots, T_\beta$. Taking the risk neutral expectation of the discounted IRS pay-off at time t with respect to $\mathcal{F}_t$, the filtration, we obtain the pricing formula of the above IRS:

$$\mathrm{P_{IRS}} = E[\mathrm{PV_{IRS}(t)}|\mathcal{F}_t] = \sum_{i=\alpha+1}^{\beta} P(t,T_i)\tau_i(F(t;T_{i-1},T_i)-K). \qquad (2.3)$$

Where $P(t,T_i)$ the zero-coupon bond price at time t, and $F(t;T_{i-1},T_i)$ the forward Libor rate at time t between T_{i-1} and T_i. Mathematically it reads as as follows:

$$F(t;T,S) = \frac{1}{S-T}\left(\frac{P(t,T)}{P(t,S)}-1\right)\ , S > T.$$

The value of fixed rate K such that the IRS has zero value is called forward swap rate which is another important rate often used in swaption valuation. The formula reads

$$S_{\alpha,\beta}(t) = \frac{P(t,T_\alpha)-P(t,T_\beta)}{\sum_{i=\alpha+1}^{\beta}\tau P(t,T_i)}. \qquad (2.4)$$

[1] We assume unit notional amount in this thesis for clarification

The derivation of the pricing formula and forward swap rate is straightforward and it is omitted in this thesis. Notice that the yield curve is necessary for IRS valuation.

2.2 Caps/Floors

An interest rate cap is basically a payer interest rate swap where the payment is made only if it has positive value. Clearly the discounted pay-off function reads

$$\mathrm{PV_{CAPS}(t)} = \sum_{i=\alpha+1}^{\beta} D(t,T_i)\tau_i \left(L(T_{i-1},T_i) - K\right)_+ . \tag{2.5}$$

Similarly, a floor is equivalent to a receiver IRS in which the payment is made when the floating rate is below a certain value. It is worth mention that a caps can be decomposed additively because the summation is outside the convex function, $()_+$. Market quotes caps using the Black's model implied volatility [9]. Caps are consist by a series of caplets and their price can be evaluated separately to derive the pricing formula below

$$\mathrm{P_{Caps}}(0, \mathrm{K}, \mathcal{T}, \tau, \sigma_{\alpha,\beta}) = \sum_{i=\alpha+1}^{\beta} P(0,T_i)\tau_i \mathrm{Bl}(K, F(0,T_{i-1},T_i), v_i). \tag{2.6}$$

With $\mathrm{Bl}(K,F,v)$ the core of Black's formula:

$$\mathrm{Bl(K,F,v)} := F\mathcal{N}(d_+(K,F,v)) - K\mathcal{N}(d_-(K,F,v)) \tag{2.7}$$

$$d_\pm(K,F,v) := \frac{\log(F/K) \pm v^2/2}{v} \tag{2.8}$$

$$v_i = \sigma_{\alpha,\beta}\sqrt{T_{i-1}}. \tag{2.9}$$

with the set of maturities: $\mathcal{T} = T_\alpha, \cdots, T_\beta$, and $\tau = \tau_{\alpha+1}, \cdots, \tau_\beta$. $\sigma_{\alpha,\beta}$ is the implied volatility which can be retrieved from the market.

2.3 Swaption

Companies enter in an interest rate swap contract to lock in a profit by receiving a fixed rate payment in exchange of paying a floating rate, or convert its fixed rate liability to an agreed floating rate liability. They choose to enter a swaption contract to manage interest rate risk arising from their core business. Swaption is the option on interest rate swap. It gives the owner the right to enter in an IRS at a predetermined fixed rate in the future. Mathematically the discounted pay-off function reads:

$$\mathrm{PV_{Swaption}(t)} = D(t,T_\alpha)\left(\sum_{i=\alpha+1}^{\beta} P(T_\alpha,T_i)\tau_i(F(T_\alpha;T_{i-1},T_i) - K)\right)_+ . \tag{2.10}$$

Noticing the summation is inside the convex function, $()_+$. This implies the join distribution of different forward rates need to be dealt with in order to price a swaption. Swaption valuation requires modelling the dynamics of interest rates which is different from caps valuation in 2.2. It is market practice to price swaption with Black-like formula [9]:

$$\mathrm{P}_{\text{Swaption}}(0, K, \mathcal{T}, \tau, \sigma_{\alpha,\beta}) = \mathrm{Bl}(K, S_{\alpha,\beta}(0), \sigma_{\alpha,\beta}\sqrt{T_\alpha}) \sum_{i=\alpha+1}^{\beta} \tau_i P(0, T_i). \tag{2.11}$$

Where $\sigma_{\alpha,\beta}$ is retrieved from the market swaption volatility surface, and $S_{\alpha,\beta}(0)$ is known as the ATM strike:

$$K_{ATM} := S_{\alpha,\beta}(0) = \frac{P(0, T_\alpha) - P(0, T_\beta)}{\sum_{i=\alpha+1}^{\beta} \tau_i P(0, T_i)}. \tag{2.12}$$

3 Literature review

In this section, we will the existing models and frameworks on caps/floors and swaption pricing and risk assessment such as the Libor market model, the SABR model, the λ-SABR model, the SABR extension to the Libor market model, the connection between models and the actual portfolio P&L calculation, the relation between P&L prediction technique and sensitivities, and the different approaches to P&L attribution.

3.1 Libor Market Model

Different components such as short rate and forward rate can be modelled in interest rate derivatives pricing. Short rate model, forward rate model and Libor market model (LMM) have been applied and tested over the years by financial institutions. Among them LMM is considered one of the most popular and promising family of interest rate model [9]. The advantage of Libor market model is each forward rate is modelled by a log-normal process under its forward measure. Moreover, cap prices are quoted in the market in terms of implied volatility which can be calculated using LMM. [13] and [16] showed that Swaptions can be managed well in the model through approximations like drift freezing. Brigo and Mercurio derived the Black's formula under the LMM assumption for caplets which turns out to match the classic market Black's formula [9]. We discuss technical detail on Libor market model in relation to the caps/floors pricing.

3.1.1 LFM

In the Log-normal Forward Libor model (LFM), forward rates are model as log-normal processes. Therefore, under the respective T_k-forward measure Q^k

$$dF_k(t) = \sigma_k(t)F_k(t)dZ_k(t),\, t \leq T_{k-1}. \tag{3.1}$$

with the set $\mathcal{E} = T_0, T_1, \cdots, T_M$ the expiry-maturity dates, $F_k(t) = F(t; T_{k-1}, T_k)$ the forward rate at time t between T_{k-1} and T_k, Z_k the k-th element of the M-dimensional Brownian motion Z under Q^k measure, and instantaneous covariance $\rho = (\rho_{i,j})_{i,j=1,\cdots,M}$

$$dZ(t)^{\intercal} dZ(t) = \rho dt.$$

3.1.2 Instantaneous Covariance Structure

Selecting appropriate instantaneous covariance structure is another topic in practice. Different forms of volatilities structures have been proposed such as general piecewise constant, separable piecewise constant, and parametric linear-exponential. The choice of the covariance structure matters the final calibration result in terms of calibration error, regular instantaneous correlation, regular terminal correlations and smoothness of the caplet volatilities' evolution over time [13]. It seems the assumption that the volatility $\sigma_k(t)$ is general piece wise constant generally performs better. This will be also discussed in the calibration of the LFM model. We clarify the mathematical definition as follows: $\sigma_k(t) = \sigma_{k,\beta(t)}$, where $\sigma_k(0) = \sigma_{k,1}$ and $t \in (T_{\beta(t)-2}, T_{\beta(t)-1]}]$. The instantaneous volatility structures thus can be specified across all the forward rates: $F_1(t), F_2(t), \cdots, F_M(t)$.

We will use another interesting structure, Parametric Linear-Exponential (LE), in the further sections on the SABR model. The advantage of this setting is that the volatility for each forward rate, F_{i-1}, can be modelled with only four parameters, and the structure satisfies that the volatility is time homogeneous, i.e. the volatility depends on the time to maturity. Mathematically the volatility $\sigma_i(t)$ reads

$$\sigma_i(t)^2 = \int_0^{T_{i-1}} [(a + b\tau_{i-1}) \exp(-c\tau_{i-1}) + d]^2 dt \quad , \tau_{i-1} = T_{i-1} - t. \tag{3.2}$$

3.1.3 Decorrelation

If we assume $\rho_{i,j} = 1$, then the correlations between forward rates are too correlated. Brigo [9] and Joshi [3] gives some insights and empirical analysis to show how to reduce the correlations between forward rates. It seems that the instantaneous correlations between forward-rates are not only the source affecting the terminal correlation between different forward rates. The instantaneous volatility specification also contributes.

Monte Carlo simulation has been suggested to study the terminal correlations of forward rates. However, it seems an approximation approach is more preferable to check the model reliability in practice. Two different versions of the approximation formula have been discussed in [13]:

$$\mathrm{Corr}(F_i(T_\alpha), F_j(T_\alpha)) = \frac{\exp(\int_0^{T_\alpha} \sigma_i(t)\sigma_j(t)\rho_{i,j} dt - 1}{\sqrt{\exp(\int_0^{T_\alpha} \sigma_i^2(t)dt) - 1}\sqrt{\exp(\int_0^{T_\alpha} \sigma_j^2(t)dt) - 1}} \tag{3.3}$$

$$\mathrm{Corr}^{\mathrm{REB}}(F_i(T_\alpha), F_j(T_\alpha)) = \rho_{i,j} \frac{\int_0^{T_\alpha} \sigma_i(t)\sigma_j(t)dt}{\sqrt{\int_0^{T_\alpha} \sigma_i^2(t)dt}\sqrt{\int_0^{T_\alpha} \sigma_j^2(t)dt}}. \tag{3.4}$$

Numerical tests against Monte Carlo simulation shows that both formulae work well in dealing with correlation approximation [13].

3.1.4 Calibration

The calibration and pricing procedure of LFM can be done in two flavours: 1) calibrate LFM with striped caps/floors volatilities from caps market quotes. 2) using the model to incorporate as many the standard market swaptions prices as possible.

The calibration of caps market prices is automatic as the caps are quotes by Black's model implied volatility. However, market quotes prices of caps instead of caplets. The common approach requires stripping caplet volatilities from cap price, and using caplet volatilities as model input [9].

The caplet price can be evaluated as:

$$\mathrm{P}_{\mathrm{Caplet}}(0,T_{i-1},T_i) = P(0,T_i)\tau_i \mathrm{Bl}(K, F(0,T_{i-1},T_i), \sqrt{T_{i-1}}v_{T_{i-1}-caplet}). \tag{3.5}$$

Where $v_{T_{i-1}-caplet}$ is the termed T_{i-1} caplet volatility, defined as the square root of the average percentage variance of the forward rate F_i(t) for $t \in [0, T_{i-1})$:

$$v^2_{T_{i-1}-caplet} := \frac{1}{T_{i-1}} \int_0^{T_{i-1}} \sigma_i(t)^2 dt. \tag{3.6}$$

In order to calibrate LFM using caplet volatilities, we need to apply a striping algorithm to produce caplets volatilities from caps quotes and plug into the model. A stripping algorithm has been mentioned in [9] and several common practical algorithms are discussed in [5] with associated statistical analysis. Recall the termed T_{i-1} caplet volatility 3.6 and apply the general piecewise constant assumption in LFM, we have in general

$$v^2_{T_{i-1}-caplet} := \frac{1}{T_{i-1}} \int_0^{T_{i-1}} \sigma_i(t)^2 dt = \frac{1}{T_{i-1}} \sum_{j=1}^{i} (T_{j-1} - T_{j-2})\sigma^2_{i,j}. \tag{3.7}$$

Assuming further that the piecewise constant volatility depends only on the time to maturity, the only parameter left to be calibrated with the swaption price is the correlation ρ. Once we approximate the forward rates correlation, the calibration process for LFM under the above assumption is then complete. Two approximation formula were derived in [9] to compute the swaptions volatility under the LFM model. It seems the difference between both formulas is negligible in non-pathological situations according to the Monte Carlo simulations test. Hence we state the simpler formula for clarification:

Rebonato's formula : The squared swaption volatility multiplied by T_α can be approximated as:

$$(v^{LFM}_{\alpha,\beta})^2 = \sum_{i,j=\alpha+1}^{\beta} \frac{w_i(0)w_j(0)F_i(0)F_j(0)\rho_{i,j}}{S_{\alpha,\beta}(0)^2} \int_0^{T_\alpha} \sigma_i(t)\sigma_j(t)dt. \tag{3.8}$$

The above formula relies on the algebraic transformations of forward rates:

$$S_{\alpha,\beta}(t) = \sum_{i=\alpha+1}^{\beta} w_i(t)F_i(t).$$

Assuming volatility is general piecewise constant and instantaneous correlations, ρ, are given exogenously, we have

$$\int_0^{T_\alpha} \sigma_i(t)\sigma_j(t)dt = \sum_{h=0}^{\alpha} (T_h - T_{h-1})\sigma_{i,h+1}\sigma_{j,h+1}.$$

If we assume other structure such as SPC parametrisation or L-E formulation for instantaneous volatilities, different parameters and calibration procedures need to be calibrated jointly with swaptions prices.

The above calibration processes manage to fit the market caps/floors or swaption data with very small error [13]. However, as suggested in [10], the volatility smile implied by the LMM are rather grid, and are not rich enough to fit the observed market caps/floors and swaptions. We naturally attempt to incorporate LMM model with stochastic volatility model.

3.2 SABR Model

Market implied volatility always varies with both the strike and the time to maturity. The SABR model attempts to capture the volatility smile structure by modelling a single forward rate with an stochastic volatility dynamics. Hagan and his co-workers has derived asymptotic formulas for the SABR model in [12]. The core result is close-form algebraic formulas for the implied volatility as functions of today's forward price and the strike.

In this section, we present the background information on the basic SABR model, and some crucial steps in the derivations of approximation formulae. Then we introduce the LMM/SABR model which combines the classic Libor market model with SABR model.

3.2.1 Model Dynamics

Based on martingale pricing theory, it is clear that the forward price F is a martingale under the forward measure. By the martingale representation theorem, we can claims that the forward rate process is defined as

$$dF(t) = C(t, \cdot)dW(t),\ F(0) = f. \tag{3.9}$$

where the coefficient $C(t, \cdot)$ is a deterministic or random process, and W is the standard Brownian motion in the forward measure. The Black model assumes the forward rate process to be a Geometric Brownian Motion: $dF(t) = \sigma F(t)dW(t)$. However, as we mentioned before, the assumption that the volatility is constant is rather realistic. Instead of modelling the volatility as a constant, SABR model models the volatility as a stochastic process. Mathematically the forward rate dynamics as below:

$$dF(t) = \sigma(t)F^{\beta}(t)dW_1(t) \qquad F(0) = f \tag{3.10}$$

$$d\sigma(t) = v\sigma(t)dW_2(t) \qquad \sigma(0) = \alpha. \tag{3.11}$$

Where the diffusion coefficient $C(t, \cdot) = \sigma(t)F^{\beta}(t)$ is CEV type, the volatility σ is random, and correlation exists between W_1 and W_2: $dW_1dW_2 = \rho dt$. It worth mentioning that market smile and skewness are usually managed by local volatility model (Dupire) before the SABR model has attracted the attention. Hagan [12] claims that the local volatility model causes inaccurate and unstable hedging as the model fail to predict the correct behaviour of the implied volatility curve. Detailed illustration can be found in the mentioned paper. Therefore the local volatility model will not be discussed in this thesis.

3.2.2 Approximation

The probability distribution associated with the SABR model is complicated and very difficult to be assessed analytically. One way to study the model's behaviour and properties is using Monte Carlo simulation. In regard to fast model implied volatility computation, Hagan and his co-workers derived an approximation analytically formula presenting the implied volatility of European call option as a function of strike and today's forward price, i.e. $\sigma(K,f)$, via singular perturbation analysis [12]:

$$\sigma(K,f) = \frac{\alpha}{(fK)^{(1-\beta)/2}\left[1+\frac{(1-\beta)^2}{24}\log^2 f/K + \frac{(1-\beta)^2}{1920}\log^4 f/K + \cdots\right]} \cdot \left(\frac{z}{x(z)}\right)$$
$$\cdot \left\{1+\left[\frac{(1-\beta)^2}{24}\frac{\alpha^2}{(fK)^(1-\beta)} + \frac{1}{4}\frac{\rho\beta v\alpha}{(fK)^(1-\beta)/2} + \frac{2-3\rho^2}{24}v^2\right]\tau + \cdots\right\}. \quad (3.12)$$

with

$$z = \frac{v}{\alpha}(fK)^{(1-\beta)/2}\log f/K$$

and x(z) is defined by

$$x(z) = \log\left\{\frac{\sqrt{1-2\rho z+z^2}+z-\rho}{1-\rho}\right\}$$

For the special case of at-the-money implied volatility, the 3.12 reduces to

$$\sigma_{ATM} = \sigma(f,f) = \frac{\alpha}{f^(1-\beta)}\left\{1+\left[\frac{(1-\beta)^2}{24}\frac{\alpha^2}{f^(2-2\beta)} + \frac{1}{4}\frac{\rho\beta\alpha v}{f^{1-\beta}} + \frac{2-3\rho^2}{24}v^2\right]\tau + \cdots\right\}. \quad (3.13)$$

Another more comprehensive version of this formula is stated in [9] to incorporate the caplet pricing. The T_i-maturity caplet implied volatility can be written as

$$\sigma(K,F_i(0)) = \frac{\alpha}{F_i(0)^{1-\beta}}\left\{1-\frac{1}{2}(1-\beta-\rho\lambda)\log\frac{K}{F_i(0)}\right.$$
$$\left. + \frac{1}{12}\left[(1-\beta)^2+(2-3\rho^2)\lambda^2\right]\log^2\frac{K}{F_i(0)} + \cdots\right\}. \quad (3.14)$$

Where

$$\lambda = \frac{v}{\alpha}f^{1-\beta}.$$

3.2.3 Estimate β

Hagan, Kumar, Lesniewski and Woodward claim that the market smile can be fitted fairly well with any specific value of β. Fitting market data to determine the exponent β is not a good practice as it has the same effect as fitting the market noise [12]. They suggest to extract β from historical observations of the "backbone", the curve that the at-the-money volatility (σ_{ATM}) traces. More specifically, from 3.13, we have:

$$\log\sigma_{ATM} = \log\alpha - (1-\beta)\log f + \log\left\{1+\left[\frac{(1-\beta)^2}{24}\frac{\alpha^2}{f^(2-2\beta)} + \frac{1}{4}\frac{\rho\beta\alpha v}{f^{1-\beta}} + \frac{2-3\rho^2}{24}v^2\right]\tau + \cdots\right\}.$$

We notice that the β can be determined by linear regression with historical $\log \sigma_{ATM}$ and $\log f$ data pairs. The third term factored by time to maturity, τ, can be ignored as its value is typically less than one or two percent [12]. Lesniewski suggested to fix one parameter among β and ρ to calibrate the other three parameters as experience shows that redundancy between the parameter β and ρ [10].

3.3 SABR-Libor Market Model

The SABR model is able to capture the volatility smile with stochastic volatility dynamics. It is natural to attempt extending the classic Libor market model by integrating the stochastic volatility model into the dynamics of Libor forward rates. Rebonato and his co-workers introduced a SABR extension on the classic LMM model [16]. Hagan and Lesniewski have worked also on extending the SABR model [10] subsequent to [12]. We highlight both of their work in this section. Different specifications and approaches have been used to develop the model.

3.3.1 Rebonato's SABR extension

Rebonato's approach relies on a natural decomposition of the stochastic part of the forward rate dynamics. This procedure breaks the stochastic term into one component only depends on the volatilities, and another component only depends on the correlations.

The forward rate f_i [2], $i = 1, 2, \cdots, N$ satisfies the following dynamics under the T_i-forward measure [2]:

$$df_i(t) = \sigma_i(t) f_i(t)^\beta dw_i(t) \tag{3.15}$$

$$d\sigma_i(t) = g_i(t) dk_i(t) \tag{3.16}$$

$$\frac{dk_i(t)}{k_i(t)} = u_{k_i}(t)dt + h_i(t)dz_i(t). \tag{3.17}$$

The model requires the volatility and the volatility of volatility to be time homogeneous, i.e: $g(t,T) = g(T-t)$ and $h(t,T) = h(T-t)$. The correlations are defined as:

$$dw_i(t)dw_j(t) = \rho_{ij}dt \tag{3.18}$$

$$dz_i(t)dz_j(t) = r_{ij}dt \tag{3.19}$$

$$dz_i(t)dw_j(t) = \phi_{ij}dt. \tag{3.20}$$

The drift term u_{k_i} is generally not zero for an arbitrary numeraire and can be derived under no-arbitrage principle. We will present the derivation starting from the general forward rate dynamics (under any forward measure) in the following section. Lesniweski's approximation method is based on this general expression.

[2] We use lower-case f instead of upper-case F to denote forward rate process in SABR model for clarification.

3.3.2 Approximation

The SABR/LMM model does not have explicit analytic closed form solution. By performing Monte Carlo simulation, one can still price caps/floors or swaptions using the SABR model dynamics. However, the procedure would be time consuming especially when dealing with large dimensional interest rate derivatives portfolio.

Analytic formulas has been derived to approximate swaption price in [11] and [10]. We outline the key derivations of Lesniewski in [10] as they help to determine the drift terms that left to be defined in the previous section. The approach is to first integrate a general stochastic volatility process on the LMM forward rates dynamics, and then apply the standard change of numeraire technique in order to determine the drift for both forward rates and the volatility process of the rates assuming SABR model's dynamics. By construction, the single forward rate SABR model has been extended to a M-dimensional forward rate model. Under a forward measure, namely T_j-forward measure, the dynamics of the forward rate $f_i(t)$ can be written as:

$$df_i(t) = \Delta_i(t)dt + C_i(t)dw_i(t) \tag{3.21}$$

Where the drift Δ_i reads:

$$\Delta_i(t) = C_i(t) \times \begin{cases} -\displaystyle\sum_{i=j+1}^{k} \frac{\rho_{ji}\tau_i\sigma_i(t)f_i(t)^{\beta_i}}{1+\tau_i f_i(t)}, & \text{if } j < k, \\ \displaystyle\sum_{i=k+1}^{j} \frac{\rho_{ji}\tau_i\sigma_i(t)f_i(t)^{\beta_i}}{1+\tau_i f_i(t)}, & \text{if } j > k, \end{cases} \tag{3.22}$$

Thus, Under the T_k-forward measure, we have

$$df_j(t) = \sigma_j(t)f_j(t)^{\beta_j} \times \begin{cases} -\displaystyle\sum_{i=j+1}^{k} \frac{\rho_{ji}\tau_i\sigma_i(t)f_i(t)^{\beta_i}}{1+\tau_i f_i(t)}dt + dw_j(t), & \text{if } j < k, \\ dw_j(t), & \text{if } j = k, \\ \displaystyle\sum_{i=k+1}^{j} \frac{\rho_{ji}\tau_i\sigma_i(t)f_i(t)^{\beta_i}}{1+\tau_i f_i(t)}dt + dw_j(t), & \text{if } j > k. \end{cases} \tag{3.23}$$

and

$$d\sigma_j(t) = \alpha_j(t)\sigma_j(t) \times \begin{cases} -\displaystyle\sum_{i=j+1}^{k} \frac{r_{ji}\tau_i\sigma_i(t)F_i(t)^{\beta_i}}{1+\tau_i F_i(t)}dt + dz_j(t), & \text{if } j < k, \\ dz_j(t), & \text{if } j = k, \\ \displaystyle\sum_{i=k+1}^{j} \frac{r_{ji}\tau_i\sigma_i(t)F_i(t)^{\beta_i}}{1+\tau_i F_i(t)}dt + dz_j(t), & \text{if } j > k. \end{cases} \tag{3.24}$$

The dynamics of swap rate is necessary for swaption pricing under SABR/LMM model. Recall the definition of the forward swap rate:

$$S_{a,b}(t) = \frac{p(t,T_a) - P(t,T_b)}{\sum_{i=a+1}^{b} \tau_i P(t,T_i)} = \frac{\sum_{i=a+1}^{b} \tau_i f_i(t) P(t,T_i)}{\sum_{i=a+1}^{b} \tau_i P(t,T_i)}. \tag{3.25}$$

Fixing a measure Q and apply Itô lemma on the forward swap rate. Substitute the forward rate dynamics with 3.23 and 3.24. And rewrite the swap rate dynamics into the form :

$$dS(t) = U(t)dt + \sum_{i=a+1}^{b} V_i(t)dW_i(t) \tag{3.26}$$

Where

$$U = \sum_{i=\alpha+1}^{b} \frac{\partial S}{\partial f_i}\Delta_i + \frac{1}{2}\sum_{a+1\leq i,j\leq b} \frac{\partial^2 S}{\partial f_i \partial f_j} C_i C_j \rho_{ij}$$

and

$$V_i = \frac{\partial S}{\partial f_i} C_i$$

The key step of above transformation is to change the measure from Q to the equivalent martingale measure Q^{ab} associated with the annuity under which the swap rate dynamics is:

$$dS(t) = \sigma(t)S(t)^{\beta}dW(t). \tag{3.27}$$

Square both 3.26 and 3.27, it is then straightforward to express the β-volatility process $\sigma(t)as$:

$$\sigma(t) = \sqrt{\sum_{a+1\leq i,j\leq b} \rho_{ij} \frac{V_i(t)}{S(t)^{\beta}} \frac{V_i(t)}{S(t)^{\beta}}}. \tag{3.28}$$

From here, Lesniewski derived an analytic approximation formula for swaption volatility using a low noise expansion approach and drift freezing technique [10]. The mentioned derivation will be introduced in the construction of the λ-SABR/LMM model. In the following section on the SABR/LMM calibration, we focus on Rebonato's work in [11] due to the simplicity and completeness of the model. Rebonato firstly proposed a curve labelled stochastic volatility approximation in [2]. Then a different approximation technique has been presented later by Rebonato and White in [11]. The new approach seems to be a better approximation according to the market case study in the later paper. We will present Rebonato's approximation technique jointly with the calibration procedure.

3.3.3 Calibration with Caplets

It is known that a cap is a series of caplets and caplet price can be evaluated separately. Because we are not dealing with correlations between forward rates, it is clear to see caps and floors price in the SABR/LMM model is consistent with the classic SABR model for each time span. The objective of calibrating LMM/SABR model with caplets is to recover the SABR caplet prices with LMM/SABR dynamics as close as possible [16].

Rebonato's approach to the approximation for caplet price relies on matching the SABR model price with the LMM/SABR model price [11], i.e.

$$E\left[\int_0^T \sigma^2_{\text{SABR}}(t)dt\right] = E\left[\int_0^T g(t)^2 k(t)^2 dt\right]. \tag{3.29}$$

By doing transformations with Fubini's theorem and Taylor expansion to match the first and second order term, we have the approximation formula for SABR model volatility with LMM/SABR volatility:

$$\alpha^2 T = k(0)^2 \int_0^T g(t)^2 dt \tag{3.30}$$

$$v = \frac{k(0)}{\alpha T} \int_0^T g(t)^2 \widehat{h}(t)^2 dt. \tag{3.31}$$

Where

$$\widehat{h}(t) = \sqrt{\frac{1}{t} \int_0^t h(s)^2 ds}.$$

Providing the classical SABR model parameters, $(\alpha_i, \rho_i, \beta_i, v_i)$, calibrated with caplets price for all the maturities T_i, the calibration procedure is then reduced to choosing the appropriate parameters for functions: $g(\cdot)$ and $h(\cdot)$ and the initial value of process k. Recall that function $g(\cdot)$ and $h(\cdot)$ are time homogeneous. This implies function $g(\cdot)$ and $h(\cdot)$ depend on the time to maturity. It is then logical to parametrize these two function using Parametric Linear-Exponential [9]. The later parametrization will also reduce the number of variables to calibrate. It seems plausible to set the expectation of SABR volatility $E[\sigma(t)] = \alpha$ to be as close as possible to the root-mean-squared value of $g(t)$ in practice [16]. The first step of the calibration is to minimize the sum of squared discrepancies:

$$\chi^2 = \sum_{i=1}^{N} E[\alpha_i - \widehat{g}(T_i)]^2. \tag{3.32}$$

Where

$$\widehat{g}(T_i) = \sqrt{\frac{1}{T_i} \int_0^{T_i} [(a + b\tau_i) \exp(-c\tau_i) + d]^2 d\tau_i}.$$

And chose $k_i(0)$ such that:

$$\alpha_i = k_i(0)\widehat{g}(Ti)$$

The calibration with caplets price is completed by using the same principle with 3.31. Note that the correlation between the Brownian motions in the forward rates, ρ, and the exponent parameter, β, are set to the same values as in the SABR model to assure the above equality.

3.3.4 Calibration with Swaptions

The SABR/LMM model will only be fully specified once the parameters in 3.15 to 3.20 are determined. The correlation structure is left to be calibrated providing the calibration with caplet prices is done. It is clear to see that the correlations among the volatilities, r_{ij}, among non-diagonal components, ϕ_{ij}, could be potentially calibrated by contingents with more complex pay-off such as swaptions. The full correlation structures is defined as:

$$\mathbf{P} = \begin{bmatrix} \boldsymbol{\rho} & \boldsymbol{\phi} \\ \boldsymbol{\phi}' & \boldsymbol{r} \end{bmatrix} \tag{3.33}$$

Rebonato demonstrated two routes to approximate the initial value of the swap rate and to approximate the swap rate volatility which determines the swaption price. Intuitions and detailed derivation can be found in [2], [11] and [16]. We simply state the key formulae used for model calibration and valuation in this thesis.

The SABR dynamics of the swap rate are defined as:

$$dS(t) = \Sigma S(t)^B dZ(t) \tag{3.34}$$

$$d\Sigma(t) = V\Sigma(t)dW(t) \tag{3.35}$$

$$\langle dZ(t), dW(t)\rangle = \phi dt. \tag{3.36}$$

Recall the basic concepts on swaption, the forward swap rate spanned by forward rate f_i to f_N can be expressed as:

$$S(t) = \sum_{i=1}^{N} w_i f_i(t).$$

Where w_i are the usual forward rate dependent weights. We can set

$$W_i(t) = w_i \frac{f_i(t)^\beta}{S(t)^B}$$

And apply drift freezing technique [9], [16] The initial value of the swap rate volatility $\Sigma(0)$ reads:

$$\Sigma(0) = \sqrt{\frac{1}{T}\sum_{1\le i,j\le N}\left(\rho_{ij}W_i(0)W_j(0)k_i(0)k_j(0)\int_0^T g_i(t)g_j(t)dt\right)}. \tag{3.37}$$

The volatility of volatility of swap rate, V, is:

$$V = \frac{1}{\Sigma(0)T}\sqrt{2\sum_{1\le i,j\le N}\left(\rho_{ij}r_{ij}W_i(0)W_j(0)k_i(0)k_j(0)\int_0^T g_i(t)g_j(t)\widehat{h}(t)^2 t dt\right)}. \tag{3.38}$$

The correlation between a swap rate and its volatility, ϕ, is approximated as:

$$\phi = \sum_{1\le i,j\le N} \Omega_{ij}\phi_{ij}$$

With the matrix Ω:

$$\Omega_{ij} = \frac{2\rho_{ij}\phi_{ij}W_i(0)W_j(0)k_i(0)k_j(0)\int_0^T g_i(t)g_j(t)\widehat{h}(t)^2 t dt}{(V\Sigma(0)T)^2}$$

The exponent B is simply set as: $B = \sum_{i=1}^N w_i\beta_i$.

3.4 λ-SABR Model

We have mentioned that the asymptotic expression is derived using singular perturbation technique as no analytical solutions are available for the SABR model. The approximation of SABR extension on Libor market model relies also on this approach. However, this seems not to be the only and the best approach. Labordère has been studied on the smile asymptotic from a different perspective in [1]. Using the heat kernel expansion on a Riemannian manifold, he managed to derive an asymptotic solutions for the implied volatility and conditional probability with general stochastic volatility model. He also claimed that the volatility is not a tradable asset, it is appropriate to model the drift under the risk neutral measure. A λ-SABR model thus has been introduced by him in [1]. The topic is relatively new and seems to be less studied comparing to classic SABR model and SABR/LMM model. Fahrner has formulated the derivation in detail using Labordère's approach [4]. In this section, we introduce the necessary definitions and state the plausible approximation formulae.

3.4.1 Geometry

We start specifying Labordère's approach by presenting the definitions structured by Fahrner in [4]. These serve as geometric foundation for the Heat Kernel Expansion approach.

Definition 3.1. Given the n-dimensional SDE system for $t \in [0, \infty)$:

$$dx_t^i = b^i(t, x_t)dt + \sigma^i(t, x_t)dW_t^i \tag{3.39}$$

$$dW_t^i dW_t^j = \rho_{ij}(t)dt \tag{3.40}$$

A *metric* $G : [0, \infty) \times \mathbb{R}^n \to \mathbb{R}^{n \times n}$, $G = (g_{ij})$ satisfies:

$$g_{ij}(t, x) = 2\frac{\rho^{ij}(t)}{\sigma^i(t, x)\sigma^j(t, x)}$$

and the inverse metric is defined as:

$$g^{ij}(t, x) = \frac{1}{2}\rho_{ij}(t)\sigma^i(t, x)\sigma^j(t, x)$$

with (ρ^{ij}) the symmetric matrix of (ρ_{ij})

Definition 3.2. The *Christoffel symbols* is : $\Gamma_{ij}^p : [0.\infty) \times \mathbb{R}^n \to \mathbb{R}$ satisfying

$$\Gamma_{ij}^p = \frac{1}{2}g^{pk}(-\partial_k g_{ij} + \partial_j g_{ki} + \partial_i g_{jk})$$

Definition 3.3. The *connection* $\mathcal{A} : [0, \infty) \times \mathbb{R}^n \to \mathbb{R}$ satisfies

$$\mathcal{A}^i(t, x) = \frac{1}{2}(b^i - g^{-1/2}\partial_j(g^{1/2}g^{ij}) \tag{3.41}$$

$$\mathcal{A}_i = g_{ij}\mathcal{A}^j \tag{3.42}$$

$$\mathcal{A}(t, x) = \mathcal{A}_i dx^i \tag{3.43}$$

define also function Q as a function of the drift b_i

$$Q = g^{ij}(\mathcal{A}_i\mathcal{A}_j - b_j\mathcal{A}_i - \partial_j\mathcal{A}_i)$$

The *Riemann tensor*

$$R^i_{jkl} = -\partial_l \Gamma^i_{kj} + \partial_k \Gamma^i_{lj} + \Gamma^i_{kr}\Gamma^r_{lj} - \Gamma^i_{lr}\Gamma^r_{kj}$$

The *Ricci tensor*

$$R_{jl} = R^i_{jil}$$

and the *scalar curvature*

$$R = g^{ij} R_{ij}$$

Definition 3.4. Given a curve parametrization $c(s) = (c^1(s), \cdots, c^n(s))$ with $c(0) = x_1$ and $c(1) = x_2$, associated length:

$$l(x_1, x_2) = \int_0^1 \sqrt{g_{ij}(c(s)) \frac{dc^i(s)}{ds} \frac{dc^j(s)}{ds}} ds$$

The *geodesics* is the curve minimizing the associated length $l(x_1, x_2)$, and the corresponding length is called *distance* $d(x_1, x_2)$. The geodesics curve $c(s)$ satisfies the *geodesics equation*

$$\frac{d^2 x^i}{ds^s} + \Gamma^i_{jk} \frac{dx^j}{ds} \frac{dx^k}{ds} = 0 \tag{3.44}$$

Note that a transformation $T : \mathbb{R}^n \to \mathbb{R}^n$ with $t = T(x)$ transform a metric as

$$g_{x^i x^j}(x) = g_{t^k t^l}(t) \frac{\partial t^k}{\partial x^i} \frac{\partial t^l}{\partial x^j}$$

The transformed distance reads: $d_x(x_1, x_2) = d_t(T(x_1), T(x_2))$

3.4.2 Heat Kernel Expansion

The Heat Kernel Expansion is one of the main tool to study the asymptotic behaviours. It also is the entry point of Labordère's approach on the implied volatility approximation. We state the main theorem used to derived the implied volatility approximation formula. Detailed proof can be found in [1].

Theorem 3.5. *Let M be a Riemannian manifold without a boundary. For every $x \in M$, there exists a complete asymptotic expansion*

$$p(x, y, \tau) = \frac{\sqrt{g(x)}}{(4\pi\tau)^{n/2}} \sqrt{\Delta(x, y)} \mathcal{P}(x, y) \exp(-\sigma(x, y)/(2\tau)) \sum_{n=1}^{\infty} a_n(x, y) \tau^n \quad , \tau \to 0 \tag{3.45}$$

with

$$a_0(x, y) = 1 \tag{3.46}$$

$$a_1(x, x) = \frac{1}{6} R + Q \tag{3.47}$$

$$\sigma(x, y) = \frac{1}{2} d^2(x, y) \tag{3.48}$$

$$\Delta(x, y) = g(x)^{-1/2} \det(-\frac{\partial^2 \sigma(x, y)}{\partial x \partial y} g(y)^{-1/2} \tag{3.49}$$

$$g(x) = \det\left[g_{ij}(x, x)\right] \tag{3.50}$$

$$\mathcal{P}(x, y) = \exp(-\int_{\mathcal{C}(x,y)} \mathcal{A}_i dx^i) \tag{3.51}$$

The detailed explanation of each term and equation is presented in [1]. Here we simply present the method to reader for understanding the approximation formulae in the next section.

3.4.3 Approximation

Recall the SDE system defined at 3.39. Denote $x = (x_i)_{i=1,2} = (f, a)$ where f is the asset, and a is the volatility. Define the initial condition as $f(0) = f_0$, $a(0) = a_0$. 3.39 can be seen as a general stochastic volatility model. By calculating the asymptotic probability using the Heat Kernel Expansion method, Labordère derived the general asymptotic implied volatility at the first-order [1] using the above stochastic volatility model specification.

$$\sigma_{\mathrm{BS}(K,\tau)} = \frac{\log(K/f_0)}{\int_{f_0}^{K} \frac{dx}{\sqrt{2g^{ff}(c)}}} \left(1 + \tau \frac{g^{ff}(c)}{12} \Big(\frac{1}{f_{av}^2} + \frac{\partial_f^2 g^{ff}(c)}{g^{ff}(c)} - \frac{3}{4} (\frac{\partial_f g^{ff}(c)}{g^{ff}(c)})^2 \Big) \right.$$
$$\left. + \frac{\tau}{2S''} \left[\frac{(g^{ff}(c))'}{g^{ff}(c)} [(\log(g\Delta\mathcal{P}^2))' - \frac{S'''}{S''}] + \frac{(g^{ff}(c))''}{g^{ff}(c)} \right] \right). \quad (3.52)$$

with c the volatility a minimizing the geodesic distance $S(a) = d^2((f,a),(f_0,a_0))$ on the Riemann surface. The above formula is very useful to approximate any stochastic volatility model. In order to derive the approximation formula, we shall state several key theorems.

In particular, Labordère's approximation seems to be better than the classic approximation formula obtained by singular perturbation approach in SABR model [1]. We now introduce the λ-SABR which has an mean reverting drift integrated in the stochastic volatility process. The dynamics are written as

$$df(t) = a(t)C(t,f)dW(t) \quad (3.53)$$
$$da(t) = \lambda(a(t) - \bar{\lambda})dt + va(t)dZ(t) \quad (3.54)$$
$$C(t,f) = f^{\beta}(t), a(0) = a_0, f(0) = f_0. \quad (3.55)$$

The derivation requires computation of the metric and the connection associated to the λ-SABR model with some substitution in the general formula 3.52. Detailed derivation is available both in [1] and [4]. Here we sate the final approximation formula of the implied volatility of λ-SABR model.

$$\sigma_{BS}(K,\tau) = \frac{\log(f_0/K)}{vol(q)}(1 + \sigma_1(f_{av})\tau) \quad (3.56)$$

with

$$q = \frac{K^{1-\beta} - f_0^{1-\beta}}{1-\beta} \quad (\beta \neq 1) \quad (3.57)$$
$$vol(q) = \frac{1}{v} \log \left(\frac{\sqrt{a_0^2 + q^2v^2 + 2qa_0v\rho}}{a_0(1-\rho)} \right) \quad (3.58)$$
$$a_m(q) = \sqrt{a_0^2 + 2a_0v\rho q + v^2q^2} \quad (3.59)$$

and

$$\sigma_1(f) = \frac{a_m^2 C(f)^2}{24}\left(\frac{1}{f^2} + \frac{2\partial_{ff}(a_m C(f))}{a_m C(f)} - (\frac{\partial_f(a_m C(f))}{a_m C(f)})^2\right) + \frac{a_0 v^2 T \log(\mathcal{P})'(a_m)(1-\rho^2)\sqrt{\cosh(d(a_m))^2 - 1}}{2d(a_m)} \quad (3.60)$$

Moreover we have $\log(\mathcal{P})'(a_m) = \log(\mathcal{P}/\mathcal{P}^{SABR})'(a_m) + \log(\mathcal{P}^{SABR})'(a_m)$ Where

$$\log(\mathcal{P}/\mathcal{P}^{SABR})'(a_m) = \frac{\lambda}{v^2}\Bigg(G_0(\theta_2(a_m), A_0(a_m), B)\theta_2'(a_m) - G_0(\theta_1(a_m), A_0(a_m), B)\theta_1'(a_m) + A_0'(a_m)\Big(G_1(\theta_2(a_m), B) - G_1(\theta_1(a_m), B)\Big)\Bigg) \quad (3.61)$$

and

$$\log(\mathcal{P}^{SABR})'(a_m) = \frac{\beta}{2(1-\rho^2)(1-\beta)}\Bigg(F_0(\theta_2(a_m), A(a_m), B)\theta_2'(a_m) - F_0(\theta_1(a_m), A(a_m), B)\theta_1'(a_m) + A'(a_m)\Big(F_1(\theta 2(a_m), A(a_m), B) - F_1(\theta 1(a_m), A(a_m), B)\Big)\Bigg) \quad (3.62)$$

with

$$G_1(x,b) = -\csc(x) + b\mathrm{Re}(\log(\tan(\frac{x}{2}))) \quad (3.63)$$

$$G_0(x,a,b) = \cot(x)\csc(x)(a+\sin(x))(1+b\tan(x)) \quad (3.64)$$

$$A_0(a_m) = -\frac{\bar{\lambda}\sqrt{1-\rho^2}}{C(f)} \quad (3.65)$$

$$A_0'(a_m) = \frac{\bar{\lambda}\sqrt{1-\rho^2(a_0\rho + vq(f))}}{C(f)^2\,(\rho(a_0 - C(f)) + vq(f))} \quad (3.66)$$

$$F_0(x,a,b) = \frac{\sin(x)}{a+\cos(x)+b\sin(x)} \quad (3.67)$$

$$F_1(x,a,b) = \frac{-2b\arctan(\frac{b+(a-1)\tan(\frac{x}{2})}{\sqrt{a^2-b^2-1}})}{(a^2-b^2-1)^{\frac{3}{2}}} + \frac{a^2+ab\sin(x)-1}{(a^2-b^2-1)(a+\cos(x)+b\sin(x))} \quad (3.68)$$

$$\theta_2(a_m) = \pi - \arctan(\frac{\sqrt{1-\rho^2}}{\rho}) \quad (3.69)$$

$$\theta_1(a_m) = -\arctan\left(\frac{a_0\sqrt{1-\rho^2}}{a_0\rho + vq(f)}\right) + \pi\mathbb{1}_{a_0\rho+vq(f)\geq 0} \quad (3.70)$$

$$\theta_1'(a_m) = \frac{a_0(vq(f)+\rho(a_0+a_m))}{v\sqrt{1-\rho^2}q(f)(2a_0\rho + vq(f))a_m} \quad (3.71)$$

$$A(a_m) = -\left(\frac{v(f_0 - f_0^{\beta}(\beta-1)q(f))}{f_0^{\beta}(\beta-1)a_m}\right) \quad (3.72)$$

$$A'(a_m) = \frac{f_0 v(a_0\rho + vq(f)) + f_0\beta a_0(\beta-1)(a_0 + v\rho q(f))}{f_0\beta(\beta-1)a_m^2(vq(f)+\rho(a_0-a_m))} \quad (3.73)$$

$$B = \frac{\rho}{\sqrt{1-\rho^2}} \quad (3.74)$$

3.5 Portfolio Valuation

In order to understand how portfolio value is calculated empirically, we introduce the notations formulated by Leif B.G. Anderson and Vladimir V. PiterBarg [7] and [8]. The objective here is to identify the key steps to process information and define mathematically the calculations of the gain and loss of a given portfolio from a modelling point of view.

Starting from collecting market observable information, define $\Theta_{mkt}(t)$ as a N_{mkt}-dimensional market vector which contains the market data observed at time t, such as the swap and future rates in the money market which are commonly used to construct yield curve. Once we have the yield curve, it is straightforward to build zero coupon bond price function of different maturities, $P(t, T)$, which is also often used as input to the model calibration process. While most of the data used in model calibration can be observed in the market, some of the addition parameters can not be seen directly, or at least the calculation of the parameters from market data is not trivial. These additional parameters are usually parameters estimated directly from the historical data. For example, the mean reversion speed κ for an asset in a stochastic volatility model, the power parameter γ in Constant Elasticity Volatility (CEV) model. Define these addition parameters as $\Theta_{prm}(t)$, and the calibrated process can be considered as a function C, satisfying:

$$\Theta_{mdl} = C(\Theta_{mkt}(t); \Theta_{prm}(t))$$

Where $\Theta_{mdl}(t)$ is the N_{mdl}-dimensional pricing model parameters vector. It worth mentioning that introducing additional information as market variable can eliminate parameters in $\Theta_{prm}(t)$ by replacing them with model parameters and calibrating them from the market vector. However, it is well known that the $\Theta_{prm}(t)$ is scarcely reduced to empty in practice as some of the parameters are naturally not easy to deduced from the market data.

It is highly likely that numerical methods are applied to deal with instrument types when analytic pricing formula is not available. Therefore an additional parameters $\Theta_{num}(t)$ is introduced to incorporate the valuation process of a given portfolio. Parameters such as size of the discretization of finite difference grids or SDE scheme are often included in the $\Theta_{num}(t)$ vector. Denoting $V(t)$ as the portfolio value at time t with n assets and function M established from chosen model with an arbitrage-free principal. The portfolio value can be evaluated as:

$$V(t) = M(\Theta_{mdl}(t); \Theta_{num}(t))$$

The overall portfolio valuation process includes the model calibration from market data and valuation using model parameters. It can be written as a function H satisfying:

$$V(t) = H(\Theta_{mkt}(t); \Theta_{prm}(t), \Theta_{num}(t))$$

The function H suggests that the portfolio value depends not only on market data but also unobservable parameters in $\Theta_{prm}(t)$ or technical parameters in $\Theta_{num}(t)$. However, these parameters are less likely to be updated dynamically comparing to the market vector. Moreover, as we are performing analysis on sensitivities in the following sections and these computations are often done intra-day, they are rather considered as static parameters than dynamic model parameters.

3.6 Risk Computation and Sensitivities

Taylor expansion is one of the fundamental risk computation methods that are applied widely in practice. The idea is to shift the market vector by a deterministic vector value $\delta = (\delta_1, \delta_2, \cdots, \delta_n)^\intercal$ and revalue the target portfolio. Then the difference of the portfolio value can be write using Taylor expansion as:

$$V(t,\delta) = H(\Theta_{mkt}(t) + \delta) \approx H(\Theta_{mkt}(t)) + \nabla^H(t) \cdot \delta + \frac{1}{2}\delta^\intercal \cdot A^H(t) \cdot \delta \tag{3.75}$$

where ∇^H is the gradient of the transfer function H and A^H the Hessian matrix. To illustrate the method with a simple example, construct portfolio with a call option in it, the gradient ∇^H contains therefore the option delta and vega, A^H contains the option gamma, volga and vanna.The computation is more complicate with interest rate derivatives and it will be explained in the following sections.

Noticing that the overall transfer function H consists of a model calibration function C and a model valuation function M based on the calibrated model parameters, by applying chain rule, we have:

$$\nabla_i^H = \frac{\partial H}{\partial x_i}\Big|_{x=\Theta_{mkt}(t)} = \sum_{j=1}^{N_{mdl}} \frac{\partial M}{\partial y_j}\frac{\partial C_j(t)}{\partial x_i}\Big|_{y=\Theta_{mdl}(t), x=\Theta_{mkt}(t)}$$

Where the gradient of function M with respect to the model parameters can be computed at first independently with the model calibration process. The second term in the right hand side is actually the Jacobian matrix for the map from market quotes to the chosen model parameters:

$$J_{j,i} = \frac{\partial C_j}{\partial x_i}$$

It is clear that, the sensitivities with respect to the market vector is evaluated at each risk computation based on the market data while the sensitivities with respect to the model parameters is evaluated at each portfolio rebalancing as they are independent of market quotes.

The above approach provides the ability of fast and stable derivatives computation when dealing with high dimensional market vector and various fixed income instrument types in practice. This so called Algorithmic Differentiation (AD) method is thus used systematically to compute numerically first order deltas. More specifically, the Jacobian matrices are calculated during model calibration process which will reduce the cost of market quotes sensitivities computation.

3.7 P&L Predict

Providing the sensitivities specified in equation 3.75, ∇^H and A^H, one can approximate the portfolio value after a short period of time h under the assumption that there is no new trades performed during this period:

$$V(t+h) \approx V(t) + \frac{\partial V(t)}{\partial t} h + \nabla^H(t) \cdot \delta + \frac{1}{2} \delta^\intercal \cdot A^H(t) \cdot \delta \tag{3.76}$$

We observe that the second term at right hand side, $\frac{\partial V(t)}{\partial t} h$ is actually the time difference h multiplied by the portfolio theta which measures the sensitivities of the portfolio value to the passage of time, aka, the time decay. The formula is know as the second order P&L predict. If the models are appropriate and hedging has be done properly, the approximation should be an accurate prediction to the actual profit and loss. In order words, the difference between right hand side and left hand side should be very small as it presents the unexplained P&L. A large unexplained P&L implies that the currently model or hedging process did not capture the high order risks.

It worth mentioning that the computation of the portfolio theta term is not trivial. Recall that the portfolio value is compute by: $V(t) = H(\Theta_{mkt}(t))$. Without peeking in the future, the expected market vector at time $t+h$ evaluated at time t can be written as:

$$\Theta^S_{mkt}(t) = \mathbb{E}[\Theta_{mkt}(t+h) | \mathcal{F}_t]$$

Using a finite difference approach, the portfolio theta reads:

$$\frac{\partial V(t)}{\partial t} = \frac{V(t+h; \Theta^S_{mkt}(t)) - V(t)}{h}$$

The empirical calculation of the term: $V(t+h; \Theta^S_{mkt}(t))$ is simply shift the market vector from $\Theta_{mkt}(t)$ to $\Theta^S_{mkt}(t)$, then reprice the portfolio after advancing the calender at time $t+h$. By shifting the market, we actually change the expansion point from $\Theta_{mkt}(t)$ to $\Theta^S_{mkt}(t)$. Thus the P&L predict formula, 3.75 can be rewritten as:

$$V(t, \delta) = H(\Theta_{mkt}(t) + \delta) \approx H(\Theta^S_{mkt}(t)) + \nabla^H(t) \cdot (\delta - \delta^S) + \frac{1}{2} (\delta - \delta^S)^\intercal \cdot A^H(t) \cdot (\delta - \delta^S)$$

With δ^S defined as the expected market movement from time t to $t+h$:

$$\delta^S := \Theta^S_{mkt}(t) - \Theta_{mkt}(t)$$

Substitute in 3.76, we have another version of P&L predict formula:

$$V(t+h) \approx V(t+h; \Theta^S_{mkt}(t)) + \nabla^H(t) \cdot (\delta - \delta^S) + \frac{1}{2} (\delta - \delta^S)^\intercal \cdot A^H(t) \cdot (\delta - \delta^S) \tag{3.77}$$

With:

$$\delta - \delta^S = \Theta_{mkt}(t+h) - \Theta_{mkt}(t) - [\Theta^S_{mkt}(t) - \Theta_{mkt}(t)] = \Theta_{mkt}(t+h) - \Theta^S_{mkt}(t)$$

Generally, this version is preferable comparing to the predict formula 3.76 mentioned before for the following reason. We advance the calender from t to $t+h$ in order to calculate the portfolio theta using a finite difference scheme. In that case, the market vector is also expected to reflect some changes. For example, while a future contract is settled with a fixed maturity, advancing h on the calender cause the time to maturity to shrink h. However market quoted swaps is usually associated with standardized time to maturities which won't be shrunk as a future contract. Since market quoted future and swap rates are often used mutually in the process of yield curve construction, the assumption that the market vector $\Theta_{mkt}(t)$ will be held fixed is not compelling under the situation mentioned above. Therefore, using expected market vector $\Theta^S_{mkt}(t)$ to calculate portfolio value at time $t+h$ is more appropriate.

While this approximation technique is widely applied in practice by support and control group within financial institutions to compute the expected portfolio value or the expect variation of the portfolio value, there are also critical studies on the performance of this classical method. Estrella [15] discussed the limitation of using Taylor approximation in the context of risk management especially when dealing with the tail distribution where the market movement is large. Fahrner [14] also derived analytically the unexplained P&L in the context of delta gamma approximation, under extreme market scenarios.

3.8 P&L Attribution

In the previous section, we've discussed several existing P$L predict technique and formula allowing practitioners to compute the expected portfolio variation after a short period of time h which is typically set to 1 business day. In practice, practitioners bump the market with different value in vector δ, for example from 10dps to 2%, and check the gain and loss on portfolio providing the sensitivities are pre-computed. This method is often used in conjunction with stress testing and scenario analysis.

Practitioners also want to understand how much each element contributes the overall P&L figures. The previous technique seems to capture this information by performing a Taylor approximation, the value of an element in δ is scaled by its contribution, the portfolio sensitivity with respect to the item in market vector. This technique is known for its fast performance of calculating expected gain and loss on portfolio using different market shift as the computation of sensitivities has been done previously in the model calibration step. However, as the market movement is known at time $t+h$, it is less logical to perform approximation using Taylor expansion to analyse the P&L by different market component.

One method to address this problem is evaluating the change in portfolio value by brute-force bumping the market with δ and revalue the positions within the portfolio. This revaluation method has been widely applied in practice and two different schemes are implemented.

3.8.1 Waterfall Explain

Starting from $\delta(0) = (0, 0, \cdots, 0)^\intercal$, adding one more component of δ at each computation, bump the market vector with it to revalue portfolio, take the difference with last calculated portfolio value, and the difference E_i will be the P&L attribution with respect to the i-th component in the market movement:

$$E_i = V(t+h; \Theta_{mkt}(t) + \delta(i)) - V(t+h; \Theta_{mkt}(t) + \delta(i-1)) \tag{3.78}$$

With

$$\delta(i) = (\delta_1, \delta_2, \cdots, \delta_i, \cdots, 0)^\intercal \ , \ i = 1, 2, \cdots, N_{mkt}$$

We also notice that, taking the sum of E_i for all the components:

$$\sum_{i=1}^{N_{mkt}} E_i = V(t+h; \Theta_{mkt}(t)+\delta(N_{mkt}))-V(t+h; \Theta_{mkt}(t)+\delta(0)) = V(t+h; \Theta_{mkt}(t+h)-V(t+h; \Theta_{mkt}(t))$$

Which is differ from the actual P&L: $V(t+h; \Theta_{mkt}(t+h)) - V(t; \Theta_{mkt}(t))$. However, with a little effort, we can adding a second term representing the time decay in to the sum to formulate the attribution formula:

$$V(t+h; \Theta_{mkt}(t+h)) - V(t; \Theta_{mkt}(t)) = \sum_{i=1}^{N_{mkt}} E_i + [V(t+h; \Theta_{mkt}(t)) - V(t; \Theta_{mkt}(t))] \tag{3.79}$$

Recall the problem when calculating the sensitivity using unshifted market vector, it is preferable to make the same adjustment on the market vector as in the section 3.7. Therefore, we have the second version of waterfall explain formula:

$$V(t+h; \Theta_{mkt}(t+h)) - V(t; \Theta_{mkt}(t)) = \sum_{i=1}^{N_{mkt}} E_i^S + [V(t+h; \Theta_{mkt}^S(t)) - V(t; \Theta_{mkt}(t))] \tag{3.80}$$

Where:

$$E_i^S = V(t+h; \Theta_{mkt}^S(t) + \delta^S(i)) - V(t+h; \Theta_{mkt}^S(t) + \delta^S(i-1))$$

and

$$\delta^S(i) = (\delta_1^S, \delta_2^S, \cdots, \delta_i^S, \cdots, 0)^\intercal \ , \ i = 1, 2, \cdots, N_{mkt}$$

The waterfall technique is able to explain entirely the change in portfolio value as the market shifts used are known and the expected market vector can also be calculated from models. However, it is clear that the value of attribution E_i could be different depends on the correlation between the market components and how the components are ordered in the market vector. The main drawback of this method is the consistency problem caused by model construction.

3.8.2 Bump and Reset

As an alternative approach, instead of calculating the attribution term by reusing the portfolio value of the last iteration, one can reset the market shift to 0 before bumping the market with the next component:

$$E_i = V(t+h; \Theta_{mkt}(t) + \delta(i)) - V(t+h; \Theta_{mkt}(t)) \tag{3.81}$$

With

$$\delta(i) = (0, 0, \cdots, \delta_i, \cdots, 0)^\intercal \ , \ i = 1, 2, \cdots, N_{mkt}$$

As a consequence, the attribution term E_i is purely generated by the market movement by the i-th component and we thus solve the consistency problem caused by correlations and model construction. However, it is also clear that a full explanation of the portfolio variation is analytically not possible via this approach. Representing the unexplained part of the actual P&L by U, we have:

$$V(t+h; \Theta_{mkt}(t+h)) - V(t; \Theta_{mkt}(t)) = \sum_{i=1}^{N_{mkt}} E_i + [V(t+h; \Theta_{mkt}(t)) - V(t; \Theta_{mkt}(t))] + U \tag{3.82}$$

We aim to explain the change in portfolio value by summing up all the components' contribution and also the portfolio value time decay. We can imagine the unexplained P&L is generated by cross-convexity terms in the market movement of the type $\partial^2 V / \partial \delta_i \delta_j$. Therefore, if the unexplained part is large, one needs to explicitly perform the bump-and-reset technique on these components in order to evaluate the attribution:

$$E_{ij} = V(t+h; \Theta_{mkt}(t) + \delta(i,j)) - V(t+h; \Theta_{mkt}(t) + \delta(i)) - V(t+h; \Theta_{mkt}(t) + \delta(j))$$

Where

$$\delta(i,j) = (0, 0, \cdots, \delta_i, 0, \cdots, 0, \delta_j, 0, \cdots, 0)^\intercal \ , \ i, j = 1, 2, \cdots, N_{mkt} \text{ and } i \neq j$$

4 LMM/λ-SABR Model

We've reviewed the mathematical specification of the classic Libor market model, the SABR model, the SABR extension to the Libor market model, their calibration procedures and the approximation formulae for caplets and swaptions. These theories and applications have been studied broadly in academia as well as in practice. We've also reviewed the λ-SABR model which extends the classic SABR with a mean reverting dynamics. This particular model seems to be less studied jointly with the Libor market model than the previous ones according to our research. The potential explanation could be: the implied volatility asymptotic relies on the Heat Kernel Expansion on Riemannian manifold which is a very technical topic and it is relatively new in quantitative finance, the SABR extension to Libor market model performs very well in practice and there is no particular reason to carrying out such heavy derivation for the new model. The first explanation is rather a fact than hypothesis whilst the second explanation could be justified by performing some empirical analysis. This part of the thesis will focus on constructing a new model combining the SABR/LMM model with the λ-SABR model and providing a feasible calibration algorithm which will be assessed in the last chapter of the thesis using actual market data.

4.1 Model Construction

Before constructing the model λ-SABR model dynamics, recall the λ-SABR dynamics with a single maturity forward rate f

$$df_t = \sigma_t df_t^\beta dw_t \tag{4.1}$$

$$d\sigma_t = \lambda(\sigma_t - \bar{\lambda})dt + v\sigma_t dz_t \tag{4.2}$$

$$dw_t dz_t = \rho dt \tag{4.3}$$

Clearly, the volatility process is mean reverting. We attempt to incorporate this model with forward rates with different maturities. Assume that, under the T_i-forward measure, the full dynamics of the forward is give by the stochastic system

$$df_t^i = C_t^i dw_t^i \tag{4.4}$$

$$d\sigma_t^i = \mu_t^i dt + \omega_t^i dz_t^i \tag{4.5}$$

where the drift and diffusion coefficients of volatility process are of the form

$$\mu_t^i = \mu^i(f_t^i, \sigma_t^i, t) \tag{4.6}$$

$$\omega_t^i = \omega^i(f_t^i, \sigma_t^i, t) \tag{4.7}$$

Therefore, the λ-SABR/LMM model corresponds to the specification

$$C_t^i = \sigma_t^i (f_t^i)^{\beta^i} \quad (4.8)$$

$$\mu_t^i = \lambda^i(\sigma_t^i - \bar{\lambda}^i) \quad (4.9)$$

$$\omega_t^i = v_t^i \sigma_t^i \quad (4.10)$$

We reuse the definition of correlation structure for SABR/LMM model 3.33

$$\mathbf{P} = \begin{bmatrix} \boldsymbol{\rho} & \boldsymbol{\phi} \\ \boldsymbol{\phi}' & \boldsymbol{r} \end{bmatrix} \quad (4.11)$$

Let us now derive the full dynamics of the λ-SABR/LMM model, i.e. the model dynamics of forward rate f_i under a different forward measure, Q_j. Notice that the only difference between the λ-SABR/LMM model with SABR/LMM model is the volatility process. We shall determine the drift and diffusion terms for σ_t^i. Assume under the Q_j measure, the dynamics of the volatility process σ^i reads

$$d\sigma_t^i = \Delta_t^i dt + \Theta_t^i dw_t^i \quad (4.12)$$

Define the following bracket operation

$$\{X, Y\}_t = \langle X, \log Y \rangle_t$$

where $\langle \cdot, \cdot \rangle$ denotes quadratic covariation. By Girsanov's theorem, we change the measure from T_i-forward measure to T_j-forward measure. Then for $i < k$ we have

$$\begin{aligned} \Delta_t^i &= \mu_t^i - d\left\{\sigma_t^i, \frac{P(\cdot, T_i)}{P(\cdot, T_j)}\right\} & (4.13)\\ &= \mu_t^i - d\left\{\sigma_t^i, \prod_{i \le k \le j} (1 + \tau_k f_k)\right\} & (4.14)\\ &= \mu_t^i - d\left\langle \sigma_t^i, \log \prod_{i \le k \le j} (1 + \tau_k f_k)\right\rangle & (4.15)\\ &= \lambda^i(\sigma_t^i - \bar{\lambda}^i) - \sigma_t^i (f_t^i)^{\beta^i} \sum_{i \le k \le j} \frac{r_{ik}\tau_k \sigma_t^k (f_t^k)^{\beta_k}}{1 + \tau_k f_t^k} & (4.16) \end{aligned}$$

Similarly, for $i > k$ we have

$$\Delta_t^i = \lambda^i(\sigma_t^i - \bar{\lambda}^i) + \sigma_t^i (f_t^i)^{\beta^i} \sum_{i \le k \le j} \frac{r_{ik}\tau_k \sigma_t^k (f_t^k)^{\beta_k}}{1 + \tau_k f_t^k} \quad (4.17)$$

Thus, the full dynamics of stochastic volatility process under T_j-forward measure can be written as

$$\sigma_t^i = \lambda^i(\sigma_t^i - \bar{\lambda}^i)dt + v_t^i \sigma_t^i \times \begin{cases} -\sigma_t^i (f_t^i)^{\beta^i} \sum_{i \le k \le j} \frac{r_{ik}\tau_k \sigma_t^k (f_t^k)^{\beta_k}}{1+\tau_k f_t^k} dt + dz_i(t), & \text{if } j < k, \\ dz_i(t), & \text{if } j = k, \\ \sigma_t^i (f_t^i)^{\beta^i} \sum_{i \le k \le j} \frac{r_{ik}\tau_k \sigma_t^k (f_t^k)^{\beta_k}}{1+\tau_k f_t^k} + dz_i(t), & \text{if } j > k. \end{cases} \quad (4.18)$$

4.2 Calibration with Caplets

Recall the calibration procedure on SABR/LMM model. Instead of minimizing the squared discrepancies between the expectation of SABR volatility α and the value of $\widehat{g}(T_i)$, we simply attempt to minimize the squared discrepancies between the expectation of $\lambda-$SABR volatility and the value of $\widehat{g}(T_i)$, i.e.

$$\chi^2 = \sum_{i=1}^{N} [\alpha_i^{\lambda-\text{SABR}} - \widehat{g}(T_i)]^2 \tag{4.19}$$

Note that this calibration procedure does not address the correlations between forward rates. We try to propose a calibration algorithm solely based on market caplets prices and provide some empirical analysis rather then study the full correlation structure. The objective is to answer the question that how the λ-SABR model performs with different forward maturities. Recall that the first step of the calibration procedure of SABR/LMM model is to recover the SABR caplet prices as close as possible with SABR/LMM dynamics. In our case, we simply replace the SABR implied volatility approximation by λ-SABR model's approximation.

4.3 Simulation Scheme

The best approach to verify the calibration result it to compare the model price with Monte Carlo simulation result which could be considered as the "true" value. We attempt to derive a simulation scheme for this purpose. Consider the process $x_t = e^{-\lambda t}\sigma_t$

$$\begin{aligned} dx_t &= -\lambda e^{-\lambda t}\sigma_t dt + e^{-\lambda t} d\sigma_t & (4.20)\\ &= -\lambda e^{-\lambda t}\sigma_t dt + e^{-\lambda t}[\lambda(\sigma_t - \bar{\lambda})dt + v\sigma_t dz_t] & (4.21)\\ &= -\lambda\bar{\lambda}e^{-\lambda t}dt + ve^{-\lambda t}\sigma_t dz_t & (4.22)\\ &= -\lambda\bar{\lambda}e^{-\lambda t}dt + vx_t dz_t & (4.23)\end{aligned}$$

The transformed process x is reduced to a linear SDE which is solvable. Let $\phi(t)$ satisfies

$$\Phi(t) = \exp\left(\int_0^t -\frac{v^2}{2}ds + \int_0^t v dz_s\right) = \exp(-\frac{v^2}{2}t + vz_t)$$

Then the solution to x reads

$$x_t = \frac{\Phi(t)}{\Phi(s)}\left(x_s + \int_s^t -\bar{\lambda}\lambda e^{-\lambda t}\frac{\Phi(s)}{\Phi(x)}dx\right) \tag{4.24}$$

Approximate $\int_s^t -\bar{\lambda}\lambda e^{-\lambda t}\frac{\Phi(s)}{\Phi(x)}dx$ by $-\bar{\lambda}\lambda e^{-\lambda s}(t-s)$ we have the simulation scheme

$$\begin{aligned} \phi &= \exp(v\Delta z - \frac{1}{2}v^2\Delta t) & (4.25)\\ x_{i+1} &= \phi(x_i - \bar{\lambda}\lambda e^{-\lambda t_i}\Delta t) & (4.26)\\ \sigma_{i+1} &= e^{\lambda(t_i+\Delta t)}x_{i+1} & (4.27)\end{aligned}$$

5 Result

We now consider some examples of calibrations specified in the literature review on SABR and LMM model. Technical details will also be presented in this section as well as the calibration result and analysis.

5.1 Data

The main financial instruments used in our calibration and analysis are interest rate caplets and swaptions. We have mentioned in the previous sections that caplets are not quoted on the money market as swaptions. Stripping algorithms are needed to retrieve caplets volatility. It is common that fixed income desks perform such algorithms to obtain caplets volatility and use it to calibrate interest rate models. These algorithms are also discussed in [5]. However, the stripping algorithms are not our main focus. Our workaround is to use cleaned caplets data from [13] and from [2] for caplets volatilities. Similarly, the entire interest rate derivatives market model calibration procedure relies on the rebuilt forward rate framework. It worth mentioning that the curve construction is also a very large topic and it is not our focus neither. Thus, we take advantage on the existing function *curve analysis* in Bloomberg Terminal. The tools allow user to retrieve Libor forward rate for give expiry time and tenor via various advanced interpolation technique. While collecting live and historical data, we also notice that Black implied volatilities are missing for certain expiry, tenor combinations on the EUR market during 2015 and 2016. The potential explanation for this issue is that the EUR market liquidity is poor in general comparing with the USD market, and it is known that the volatility structure has been changed immensely since 2015 [17]. In order to carry out consistent analysis on the SABR model and Libor market model, we select the historical USD swaptions data on 8 August 2007 which seems to be relatively mild and appropriate to study the model behaviour in general.

5.2 Market Case: LFM

As discussed in Section 3.1.4, the calibration of LFM model is done in two flavours: caplets volatility calibration and swaptions volatility matrix calibration. Model parameters can easily be calibrated with caplets volatility, however the swaption volatility is necessary to capture the correlations between forward rates between various expiry and tenor data pairs.

5.2.1 Calibration with Caplets

The calibration to caplets for LFM model is straightforward as one can use the market implied volatility as input, and the parametrization is done by minimizing the difference discrepancies between model volatility output and market volatility. Here, we carry out the LE parametrization calibration with caplets volatilities using the formula 3.6. Empirically, the model parameter $\Theta = (a, b, c, d)$ can be expressed as follows

$$\Theta = \arg\min_{a,b,c,d} \sum_{i=0}^{M} [\sigma_{\mathrm{BS}}^2 T_i - \sigma(T_i; a, b, c, d)]^2, \tag{5.1}$$

where $\sigma(\cdot)$ the L-E parametrization function of volatility depends on the expiry, and parametrized by Θ. To clarify, in this particular market case, we also want to tight the parametrization by setting the constraint on θ, the *correlation angle*

$$-\pi/3 < \theta_i - \theta_{i-1} < \pi/3, \quad 0 < \theta_i < \pi,$$

This chosen values are obtained by experimenting different possibilities to fit market data with less correlation between forward rates. The full correlation calibration is discussed further in the next step on swaption calibration. The caplets implied volatilities used in the following calibration are listed as in the Table 1.

F_0	σ_{BS}
0.050114	0.180253
0.055973	0.191478
0.058387	0.186154
0.060027	0.177294
0.061315	0.167887
0.062779	0.158123
0.062747	0.152688
0.062926	0.148709
0.062286	0.144703
0.063009	0.141259
0.063554	0.137982
0.064257	0.134708
0.064784	0.131428
0.065312	0.128148
0.063976	0.127100
0.062997	0.126822
0.061840	0.126539
0.060682	0.126257
0.059360	0.125970

Table 1: Stripped caplets volatility

Our calibration results seem to be plausible. We obtain 0.0003142 as error with $a = 0.26017369, b = 0.90896012, c = 0.10348463, d = 0.0046227$ as model parameters. In order to assess the goodness of fit of model parameters, we examine the evolution of the term structure of volatility implied by such parametrization. The term structure of volatility at time T_i is actually the plot of expiry times T_{j-1} against the average volatility $V(T_i, T_{j-1})$ of the forward rates F_j up to the expiry time. Mathematically, it is defined as follows

$$V^2(T_i, T_{j-1}) = \frac{1}{T_i - T_{j-1}} \int_{T_i}^{T_{j-1}} \sigma_j^2(t) dt,$$

where σ_j is specified by the LFM model for expiry T_j. One should expect a smooth evolution of the model volatility over time.

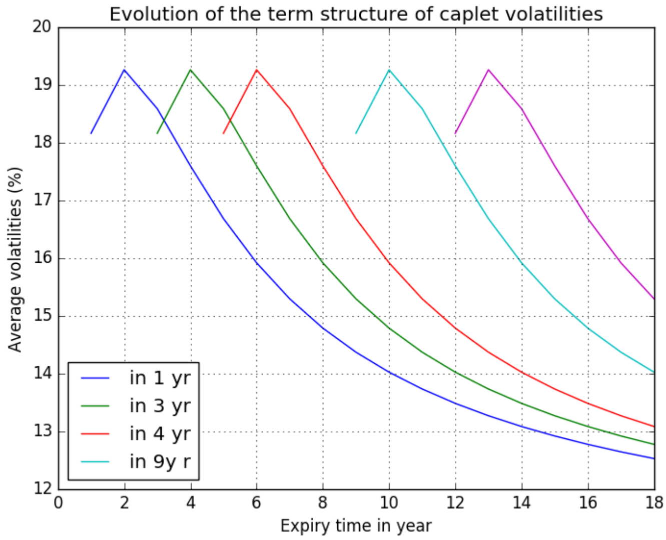

Figure 1: Evolution of the term structure of caplets volatilities

We observed in Figure 1 the "head" (between 0 and the first expiry) of each volatility term structure. This is expected as the volatility term structure suppose to remain the same between time 0 and the first expiry point. It is expected to be shorter as the time passed as the number of possible expiries has decreased by one.

5.2.2 Calibration with Swaption

We now proceed to the calibration with swaption volatility matrix. Table 2 includes the swpation volatilities quoted by expiry (row), and tenor (column) both in year. We observed firstly the value of maturities and tenors match exactly with each other. However, it is generally not the case in most of the market data provider. For example, in Bloomberg Terminal/SWAP Manager, the expiry time spans are typically 3 months, 6 months, 9 months, one year, etc, where the tenors are generally presented in year. The data used in this section is actually after preprocessing [9]. The reason is that we can present the volatility matrix in squared matrix in order to match the correlation matrix dimension to study the correlations between forward rates.

	1y	2y	3y	4y	5y	6y	7y	8y	9y	10y
1y	0.180	0.167	0.154	0.145	0.138	0.134	0.130	0.126	0.124	0.122
2y	0.181	0.162	0.145	0.135	0.127	0.123	0.120	0.117	0.115	0.113
3y	0.178	0.155	0.137	0.125	0.117	0.114	0.111	0.108	0.106	0.104
4y	0.167	0.143	0.126	0.115	0.108	0.105	0.103	0.100	0.098	0.096
5y	0.154	0.132	0.118	0.109	0.104	0.104	0.099	0.096	0.094	0.092
6y	0.147	0.127	0.113	0.104	0.098	0.098	0.094	0.092	0.090	0.089
7y	0.140	0.121	0.107	0.098	0.092	0.091	0.089	0.087	0.086	0.085
8y	0.137	0.117	0.103	0.095	0.089	0.088	0.086	0.084	0.083	0.082
9y	0.133	0.114	0.100	0.091	0.086	0.085	0.083	0.082	0.081	0.080
10y	0.130	0.110	0.096	0.088	0.083	0.082	0.080	0.079	0.078	0.077

Table 2: Swaption volatility matrix

The LFM model calibration with swaption volatilities is fairly simple once we understand the theory. As discussed in the literature review, the correlation structure between forward rates seem to be complex, and it implies that swaption volatilities of different tenor can not be calibrated together for each maturities. However, leveraging on the "drift freezing" technique, the formula proposed by Rebonato [2] makes the calibration simpler and handy. The practice is to minimize the squared error between the model implied volatility by approximation and the market quoted volatility. In this section, we shall go through several calibration key steps rather than perform the actual swaption calibration. The detail of swaption calibration will be presented and results will be analysed in the following section on SABR model calibration.

We mentioned in the literature review on the LFM model, the full calibration of LFM model requires the correlation structure between forward rates to be calibrated. To address this issue, decorrelation procedure also has been discussed. To incorporate the decorrelation with the model calibration, it is market practice to consider the constraint on the *correlation angle* [2]. The idea is to specify the correlation between two forward rates by a M rank matrix B, i.e.

$$dW(t) = BdZ(t),$$

where W and Z are both m-dimensional standard Brownian motion which are used in the forward rates dynamics. Therefore we can parametrize the M ranked matrix B by a set of correlation angles. For example, for $m = 2$, we have

$$b_{i,1} = \cos\theta_i \quad (5.2)$$

$$b_{i,2} = \sin\theta_i \quad (5.3)$$

$$\rho_{i,j} = b_{i,1}b_{j,1} + b_{i,2}b_{j,2} = \cos(\theta_i - \theta_j), \quad (5.4)$$

Rebonato's terminal-correlation formula 3.4 is used to construct the optimization problem for model calibration. We first apply the formula to compute the target correlation matrix, Table 3.

	1y	2y	3y	4y	5y	6y	7y	8y	9y	10y
1y	1.0000	0.9756	0.9524	0.9304	0.9094	0.8894	0.8704	0.8523	0.8352	0.8188
2y	0.9756	1.0000	0.9756	0.9524	0.9304	0.9094	0.8894	0.8704	0.8523	0.8352
3y	0.9524	0.9756	1.0000	0.9756	0.9524	0.9304	0.9094	0.8894	0.8704	0.8523
4y	0.9304	0.9524	0.9756	1.0000	0.9756	0.9524	0.9304	0.9094	0.8894	0.8704
5y	0.9094	0.9304	0.9524	0.9756	1.0000	0.9756	0.9524	0.9304	0.9094	0.8894
6y	0.8894	0.9094	0.9304	0.9524	0.9756	1.0000	0.9756	0.9524	0.9304	0.9094
7y	0.8704	0.8894	0.9094	0.9304	0.9524	0.9756	1.0000	0.9756	0.9524	0.9304
8y	0.8523	0.8704	0.8894	0.9094	0.9304	0.9524	0.9756	1.0000	0.9756	0.9524
9y	0.8352	0.8523	0.8704	0.8894	0.9094	0.9304	0.9524	0.9756	1.0000	0.9756
10y	0.8188	0.8352	0.8523	0.8704	0.8894	0.9094	0.9304	0.9524	0.9756	1.0000

Table 3: Target correlation matrix computed by Rebonato's formula

Table 4 presents the fitting error using Rebonato's formula. We observe that the error is less than 2% in absolute value which is expected in general. The full correlation structure is now specified by the matrix ρ and its parameters θ, thus complete the LFM model calibration.

	1y	2y	3y	4y	5y	6y	7y	8y	9y	10y
1y	0.00%	-0.16%	-0.54%	-1.13%	-1.67%	-1.87%	-1.54%	-0.96%	-0.34%	0.09%
2y	-0.16%	0.00%	-0.12%	-0.56%	-1.18%	-1.83%	-1.86%	-1.53%	-0.95%	-0.33%
3y	-0.54%	-0.12%	0.00%	-0.16%	-0.67%	-1.52%	-1.86%	-1.84%	-1.46%	-0.86%
4y	-1.13%	-0.56%	-0.16%	0.00%	-0.19%	-0.96%	-1.52%	-1.86%	-1.84%	-1.46%
5y	-1.67%	-1.18%	-0.67%	-0.19%	-0.00%	-0.37%	-0.92%	-1.49%	-1.85%	-1.85%
6y	-1.87%	-1.83%	-1.52%	-0.96%	-0.37%	-0.00%	-0.16%	-0.63%	-1.23%	-1.71%
7y	-1.54%	-1.86%	-1.86%	-1.52%	-0.92%	-0.16%	0.00%	-0.16%	-0.63%	-1.23%
8y	-0.96%	-1.53%	-1.84%	-1.86%	-1.49%	-0.63%	-0.16%	0.00%	-0.16%	-0.63%
9y	-0.34%	-0.95%	-1.46%	-1.84%	-1.85%	-1.23%	-0.63%	-0.16%	0.00%	-0.16%
10y	0.09%	-0.33%	-0.86%	-1.46%	-1.85%	-1.71%	-1.23%	-0.63%	-0.16%	0.00%

Table 4: Percentage error of correlation calibration

By carrying out the swaption calibration on different tenors, Brigo [9] also claimed that the calibration shows several negative signs in instantaneous volatilities. This is due to the "temporal misalignments" caused by illiquidity in the swaption matrix. We shall also examine this issue in-line with the SABR model calibration in the next empirical study. Here, we present a matrix smoothness technique to address this issue. Fit the swaption volatility surface into the following parametric form [13]

$$\sigma_{\text{BS}}(S,T) = \gamma(S) + \left(\frac{\exp(f \cdot \log T)}{e \cdot S} + D(S)\right) \cdot \exp(-\beta \cdot \exp(p \cdot \log T)) \quad (5.5)$$

$$\gamma(S) = c + (\exp(h \cdot \log S) \cdot a + d) \cdot \exp(-b \cdot \exp(m \log S)) \quad (5.6)$$

$$D(S) = (\exp(g \cdot \log(S)) \cdot q + r) \cdot \exp(-s \cdot \exp(t \cdot \log S)) + \delta, \quad (5.7)$$

where S is the tenor and T is the expiry time. By carrying out such smooth parametrization, the negative instantaneous volatilities issue seems to be resolved during the volatility surface calibration.

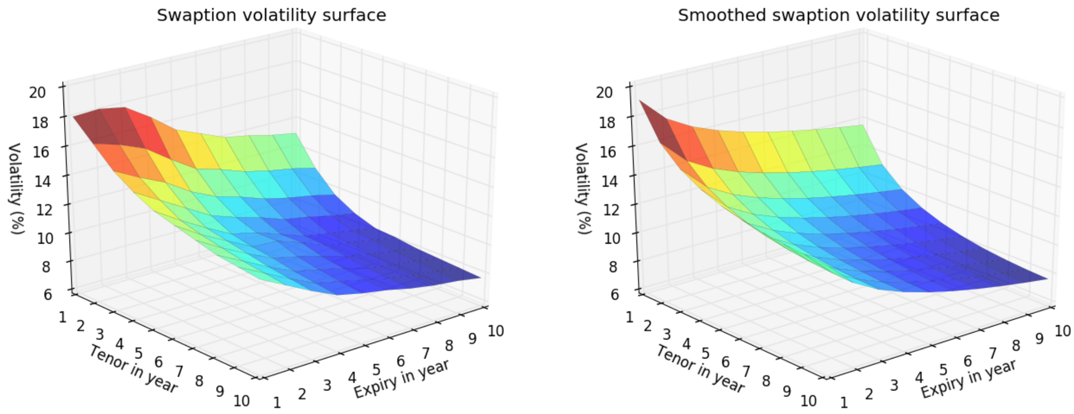

(a) Swaption volatility surface (b) Smoothed volatility matrix

Figure 2: Swaption volatility matrix smoothing

However, we notice in the Figure 2 and also in the fitting error Table 5, the edge part where the volatility surface has irregular shape is also be smoothed along with the parametrization. For example, the smooth procedure has increased the volatility of a 1-year swaption with one year tenor by 6.26%. The consequence of such behaviour is worth discussing. Intuitively, it is normal that the implied volatility at the edge of the surface is low as we are approaching the expiry. The smoothness procedure somehow adjust the volatility surface in the opposite direction which potentially causes loss of precision in pricing.

	1y	2y	3y	4y	5y	6y	7y	8y	9y	10y
1y	6.26%	0.45%	0.77%	1.51%	2.69%	2.90%	3.99%	5.81%	6.53%	7.69%
2y	-3.58%	-6.77%	-4.49%	-3.34%	-1.56%	-1.47%	-1.25%	-0.31%	0.36%	1.50%
3y	-7.44%	-8.85%	-6.03%	-3.40%	-1.46%	-2.23%	-2.01%	-1.01%	-0.30%	0.92%
4y	-5.48%	-6.02%	-3.29%	-1.00%	0.37%	-0.41%	-1.09%	0.01%	0.81%	2.15%
5y	-0.97%	-2.24%	-1.26%	-0.44%	-0.90%	-4.59%	-2.49%	-1.38%	-0.58%	0.79%
6y	0.77%	-1.82%	-0.75%	0.15%	0.72%	-3.19%	-1.94%	-1.83%	-1.00%	-0.70%
7y	3.18%	0.00%	1.37%	2.53%	3.29%	0.21%	-0.56%	-0.41%	-0.68%	-0.36%
8y	3.11%	0.70%	2.22%	2.41%	3.19%	0.01%	-0.80%	-0.65%	-0.92%	-0.60%
9y	4.10%	0.88%	2.48%	3.83%	3.52%	0.24%	-0.59%	-1.65%	-1.94%	-1.62%
10y	4.56%	2.27%	4.13%	4.52%	4.24%	0.84%	-0.00%	-1.09%	-1.39%	-1.04%

Table 5: Percentage error of volatility matrix smoothing

Readers familiar with equity option may also detect that the structure of the swaption volatility surface is different from the traditional volatility surface in the equity world, i.e. the volatility surface plotted as function of option strike and time to maturity. Instead of option strike, the at-the-money (ATM) interest rate swaption volatility surface is presented a function depending on the tenor. Actually, the swaptions volatility is a function of the expiry time, the tenor and the strike. Thus, it can be seen as a volatility cube. The above volatility surface is the slice where the swaption strike is equal to the current forward rate. It is then clear that the LFM model calibration which relies on the ATM swaption matrix does not address the issue of volatility smile where the option strikes are involved.

5.3 Market Case: SABR Model

We have introduced the SABR model which is designated to capture the volatility smile in the first part of the thesis. Before carrying out the SABR model calibration on the real market data, we devote this section to study the impact of each model parameter for the sake of preparation. The analysis will based on the plots produced by bumping gradually each of the model parameters. The parameter values used in this section are retrieved from [2]. They correspond a set of US market input on 6th April 2006.

5.3.1 Dependence on α

As seen in Figure 3, by increasing α, the Black implied volatility has also been shifted upward. This result is not surprising as we recall that the parameter α corresponds the expectation at time 0 of the stochastic volatility process σ.

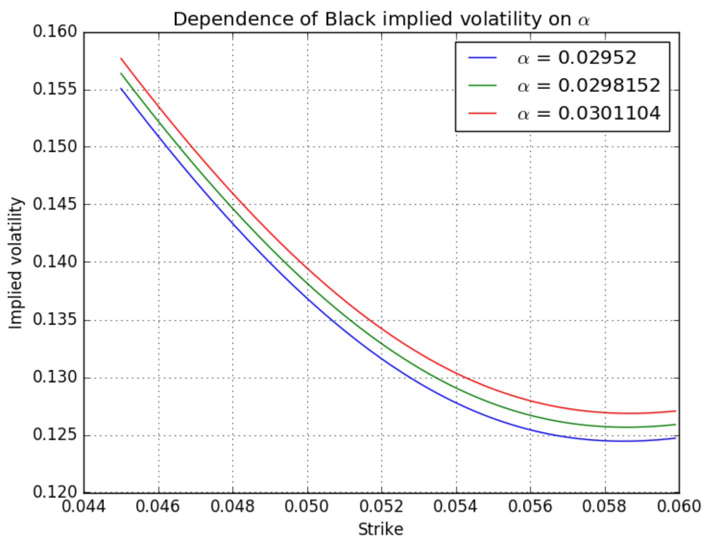

Figure 3: Black implied volatility

We also notice that as a small effect, the shift in parameter α produced more change in value on the ATM volatility than the variation at wings.

5.3.2 Dependence on β

We observe in the Figure 4 that decreasing the value of β will produce mainly a progressive steepening of the volatility smile. As the β decreases, the volatility level has raises. We recall the SABR model dynamics on the forward rate $df_t = \sigma_t(f_t)^\beta dw_t$. Intuitively, if we consider the term $\sigma_t(f)^\beta$ as the "total" volatility of the forward rate process, it is then easy to see that by decreasing the value of β, the volatility will generally magnified. We also want to mention the below figure is produced with the constraint that the value of $\sigma_t(f_t)^\beta$ remains the same in order to maintain the overall volatility level.

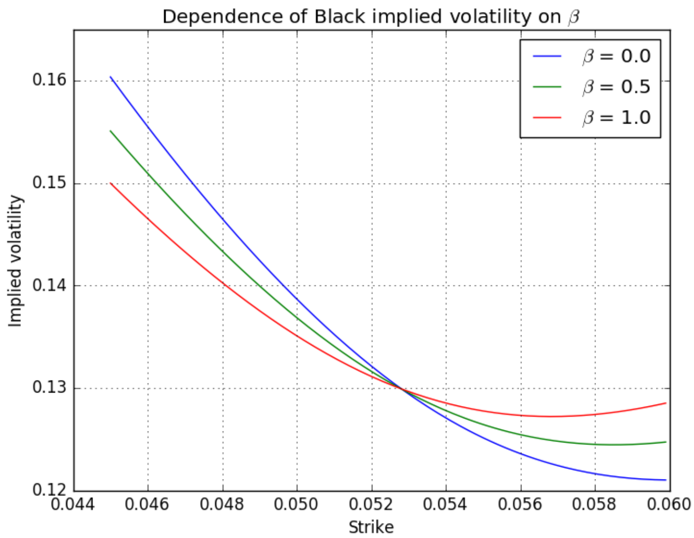

Figure 4: Black implied volatility

It is market practice to chose 0.5 as the value for β. We have also provided background information on a linear regression approach derived from the approximation formula proposed by Hagan [12] in the literature review. To be more rigorous on the choice of β, Rebonato [2] have refitted the swaptions market prices setting $\beta = 0$ and compared with the result setting $\beta = 0.5$. According to the plots of the evolution of the fitted parameter, ρ, the choice of $\beta = 0$ causes ρ to become less stable than setting β to 0.5. This choice of the β value is not optimal as SABR model assume the four parameters to be constant over time. We shall see in the following section that the change in parameter ρ has similar effect on the volatility smile. It is then logical to fix the β value to 0.5 at calibration to avoid fitting similar parameters at the same time.

Another impact on the volatility smile caused by changing β value can be observed at the lower strike, the volatility fall more rapidly than the higher strike increase. This is known as the *curvature* effect.

5.3.3 Dependence on ρ

ρ is the only parameter that allows to be fitted at negative value. We thus plot the dependence graphs separately for the positive correlation case and negative correlation case.

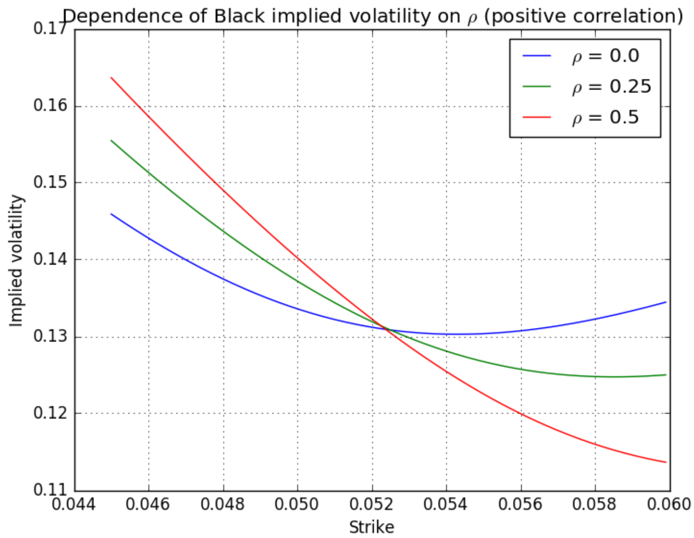

Figure 5: Black implied volatility

As seen in Figure 4 and 5, changing ρ produces similar effect on the volatility smile to β. Increasing ρ increases the steepness of the volatility smile in the positive correlation case while the opposite effect will be produced in the negative correlation case. We notice specially in the negative correlation case, Figure 6, the volatility smile becomes more and more negatively sloped.

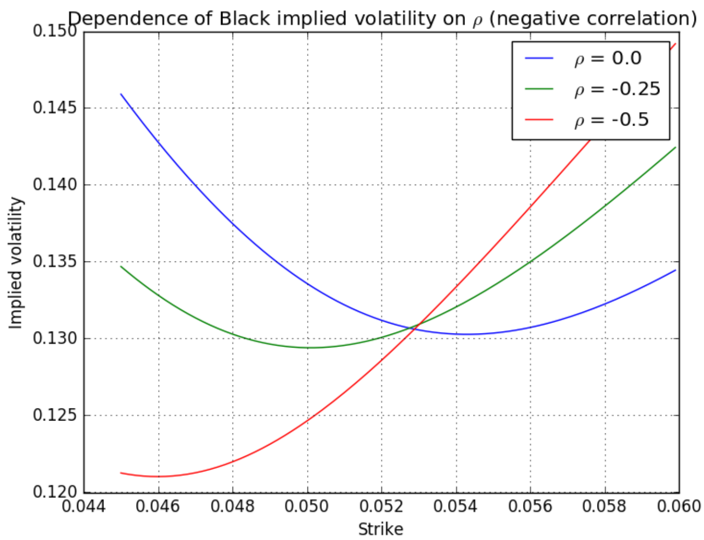

Figure 6: Black implied volatility

5.3.4 Dependence on v

Figure 7 shows that changing in v will mainly cause the curvature impact other than the steepness or the level of the volatility smile. The smile tends to be more convex when v becomes larger.

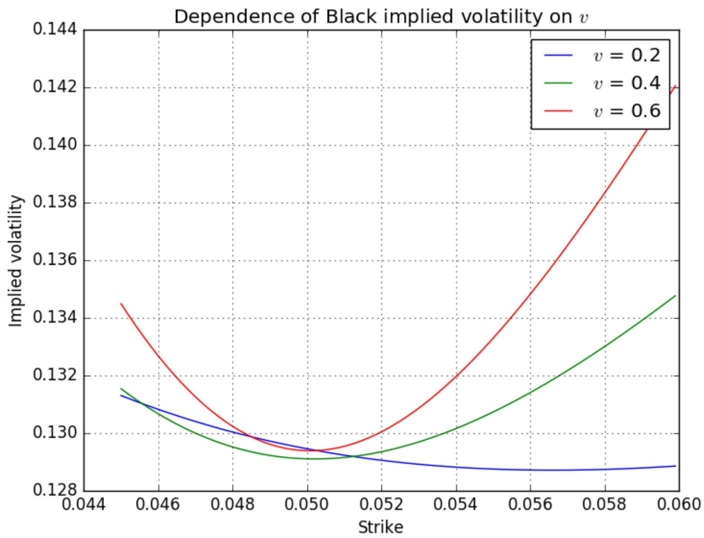

Figure 7: Black implied volatility

To sum up, the interaction between these four parameters manages to model different volatility shapes fairly well in terms of the smile level, steepness and curvature. Particularly, as changing in β and ρ produces very similar effect, and the historical data analysis shows that 0.5 seems to be an appropriate choice of the β value, we shall proceed our SABR model calibration by setting $\beta = 0.5$.

The classic SABR model does not address the join distribution of the forward rates. Similar to the LFM model, the calibration of the SABR model also requires minimization procedure for each maturity and tenor pairs. That is to say, the calibration of the whole swaption matrix will generally produce $m \times n \times 3$ parameters where m is the dimension of the forward rates, and n is the number of different tenors. In the following section, we also apply another practice using the at-the-money implied volatility as input to compute the parameter α on the fly. By doing this, only ρ and v are left to be calibrated.

5.3.5 SABR calibration with swaption

The minimization problem to be solved by SABR model calibration is matching the market implied volatility with the SABR volatility evaluated for a given strike set and current forward rate for each maturity and each tenor. Empirically, the model parameter $\Theta = (\rho, v)$ satisfies

$$\Theta = \underset{\rho, v}{\operatorname{argmin}} \sum_{i=0}^{N_k} [\sigma_{\text{BS}} - \sigma_{\text{SABR}}(f, \sigma_{\text{ATM}}, k_i, T; \rho, v)]^2, \tag{5.8}$$

The index for the expiry and tenor have been omitted for the sake of clarification. The at-the-money implied volatility has been used as input to calculate the α parameter on the fly by solving the formula 3.13 for α to speed up the calibration process. Table 6 includes the strike value for each expiry time and each tenor. Notice that the strike value for a given expiry time and tenor matches the current forward price. To be more clear, we only need one cell within the matrix to calibrate a volatility smile, one column is enough to calibrate the entire volatility surface [3].

	1y	2y	3y	4y	5y	6y	7y	8y	9y	10y	12y	15y	20y	25y	30y
1m	0.052	0.052	0.052	0.053	0.053	0.054	0.054	0.055	0.055	0.056	0.056	0.057	0.057	0.057	0.057
3m	0.051	0.051	0.052	0.053	0.053	0.054	0.054	0.055	0.055	0.056	0.056	0.057	0.057	0.057	0.057
6m	0.050	0.051	0.052	0.053	0.053	0.054	0.054	0.055	0.055	0.056	0.056	0.057	0.057	0.057	0.058
9y	0.050	0.051	0.052	0.053	0.054	0.054	0.055	0.055	0.056	0.056	0.057	0.057	0.058	0.058	0.058
1y	0.051	0.052	0.053	0.053	0.054	0.055	0.055	0.056	0.056	0.056	0.057	0.057	0.058	0.058	0.058
2y	0.053	0.054	0.054	0.055	0.056	0.056	0.056	0.057	0.057	0.057	0.058	0.058	0.058	0.058	0.058
3y	0.055	0.055	0.056	0.056	0.057	0.057	0.057	0.058	0.058	0.058	0.058	0.059	0.059	0.059	0.059
4y	0.056	0.057	0.057	0.057	0.058	0.058	0.058	0.058	0.059	0.059	0.059	0.059	0.059	0.059	0.059
5y	0.057	0.058	0.058	0.058	0.058	0.059	0.059	0.059	0.059	0.059	0.060	0.060	0.059	0.059	0.059
6y	0.058	0.058	0.059	0.059	0.059	0.059	0.060	0.060	0.060	0.060	0.060	0.060	0.060	0.059	0.059
7y	0.059	0.059	0.059	0.059	0.060	0.060	0.060	0.060	0.060	0.060	0.060	0.060	0.060	0.060	0.059
8y	0.059	0.059	0.060	0.060	0.060	0.060	0.060	0.060	0.060	0.060	0.060	0.060	0.060	0.060	0.059
9y	0.060	0.060	0.060	0.060	0.060	0.060	0.060	0.060	0.060	0.060	0.060	0.060	0.060	0.060	0.059
10y	0.060	0.060	0.061	0.061	0.060	0.061	0.061	0.061	0.060	0.060	0.060	0.060	0.060	0.059	0.059
12y	0.061	0.061	0.060	0.061	0.061	0.061	0.061	0.060	0.060	0.060	0.060	0.060	0.059	0.059	0.059
15y	0.062	0.062	0.061	0.061	0.060	0.060	0.060	0.060	0.060	0.059	0.059	0.059	0.059	0.058	0.060
20y	0.060	0.060	0.059	0.058	0.058	0.058	0.058	0.058	0.058	0.058	0.058	0.058	0.057	0.059	0.060
25y	0.060	0.060	0.059	0.058	0.058	0.058	0.059	0.059	0.058	0.058	0.058	0.057	0.060	0.060	0.057
30y	0.062	0.061	0.060	0.060	0.059	0.058	0.058	0.057	0.057	0.056	0.059	0.061	0.062	0.057	0.053

Table 6: Swaption strike matrix

In our case study, we use the one year tenor swaption volatility matrix, Table 7, for calibration. Our objective is to calibrate the volatility surface for one year tenor swaption only. To calibrate the whole volatility cube requires carrying out n times the same procedure which is not our interest.

[3]Here the volatility surface is the transitional volatility surface as a function of the expiry and strike

	1y	2y	3y	4y	5y	6y	7y	8y	9y	10y	11y	12y	13y	14y	15y	16y	17y	18y
1m	0.150	0.224	0.201	0.187	0.177	0.170	0.164	0.159	0.151	0.146	0.141	0.137	0.134	0.131	0.129	0.127	0.125	0.123
3m	0.161	0.239	0.216	0.201	0.190	0.182	0.175	0.170	0.162	0.156	0.151	0.147	0.143	0.141	0.138	0.136	0.134	0.132
6m	0.169	0.249	0.224	0.209	0.198	0.190	0.183	0.178	0.169	0.163	0.158	0.154	0.151	0.148	0.145	0.143	0.141	0.139
9y	0.174	0.256	0.231	0.215	0.204	0.195	0.188	0.183	0.174	0.168	0.163	0.159	0.155	0.152	0.150	0.147	0.145	0.143
1y	0.181	0.461	0.379	0.324	0.283	0.252	0.228	0.208	0.182	0.169	0.164	0.164	0.166	0.168	0.171	0.174	0.176	0.179
2y	0.177	0.461	0.379	0.324	0.284	0.253	0.229	0.209	0.182	0.168	0.162	0.161	0.163	0.165	0.168	0.170	0.173	0.176
3y	0.171	0.468	0.384	0.327	0.286	0.254	0.229	0.208	0.180	0.164	0.159	0.158	0.160	0.163	0.167	0.170	0.173	0.176
4y	0.164	0.451	0.370	0.316	0.276	0.246	0.221	0.202	0.174	0.159	0.152	0.151	0.152	0.155	0.158	0.161	0.164	0.166
5y	0.163	0.446	0.366	0.314	0.275	0.245	0.222	0.203	0.175	0.160	0.153	0.151	0.152	0.155	0.158	0.161	0.164	0.166
6y	0.156	0.426	0.350	0.300	0.264	0.235	0.213	0.195	0.169	0.153	0.146	0.144	0.145	0.147	0.149	0.152	0.155	0.157
7y	0.154	0.429	0.352	0.301	0.264	0.236	0.213	0.195	0.168	0.153	0.145	0.143	0.143	0.145	0.148	0.150	0.153	0.156
8y	0.146	0.420	0.343	0.293	0.257	0.228	0.206	0.188	0.161	0.146	0.138	0.135	0.136	0.138	0.140	0.143	0.145	0.148
9y	0.141	0.404	0.330	0.282	0.247	0.220	0.199	0.181	0.156	0.141	0.133	0.130	0.130	0.132	0.133	0.136	0.138	0.140
10y	0.141	0.393	0.322	0.276	0.242	0.217	0.196	0.179	0.155	0.141	0.133	0.131	0.131	0.133	0.135	0.137	0.139	0.142
12y	0.137	0.388	0.318	0.272	0.239	0.214	0.193	0.177	0.153	0.138	0.131	0.128	0.128	0.129	0.131	0.134	0.136	0.138
15y	0.135	0.385	0.314	0.269	0.236	0.211	0.191	0.175	0.151	0.137	0.129	0.125	0.125	0.126	0.128	0.130	0.132	0.134
20y	0.134	0.381	0.308	0.262	0.230	0.205	0.186	0.171	0.148	0.134	0.127	0.123	0.122	0.123	0.124	0.126	0.128	0.130
25y	0.132	0.379	0.304	0.258	0.226	0.202	0.183	0.168	0.146	0.133	0.125	0.122	0.122	0.123	0.124	0.126	0.128	0.130
30y	0.132	0.401	0.316	0.266	0.232	0.207	0.187	0.171	0.148	0.134	0.124	0.119	0.117	0.116	0.116	0.117	0.118	0.119

Table 7: Volatility matrix of swaptions with one year tenor

We obtain the following values for the model parameters in Table 8, along with the plots of implied volatility surface and the SABR fitted surface in Figure 8. Let us look at the first column of the model parameters α. The variation on α is small across different expiry time. This is also explainable by the flatness of the volatility surface especially at the large expiry part. Overall the SABR parameters capture fairly well the left side of the volatility where the expiry time is relatively small.

Expiry	α	β	rho	v
1m	0.034	0.500	0.119	0.060
3m	0.036	0.500	0.117	0.065
6m	0.038	0.500	0.150	0.068
9y	0.039	0.500	0.154	0.070
1y	0.041	0.500	-0.369	0.371
2y	0.041	0.500	-0.362	0.362
3y	0.040	0.500	-0.349	0.373
4y	0.039	0.500	-0.353	0.350
5y	0.039	0.500	-0.328	0.338
6y	0.037	0.500	-0.137	0.315
7y	0.037	0.500	-0.005	0.246
8y	0.036	0.500	-0.354	0.309
9y	0.034	0.500	-0.367	0.293
10y	0.034	0.500	-0.328	0.281
12y	0.034	0.500	-0.327	0.270
15y	0.033	0.500	-0.346	0.260
20y	0.033	0.500	-0.382	0.247
25y	0.032	0.500	-0.373	0.238
30y	0.033	0.500	-0.472	0.247

Table 8: SABR parameters

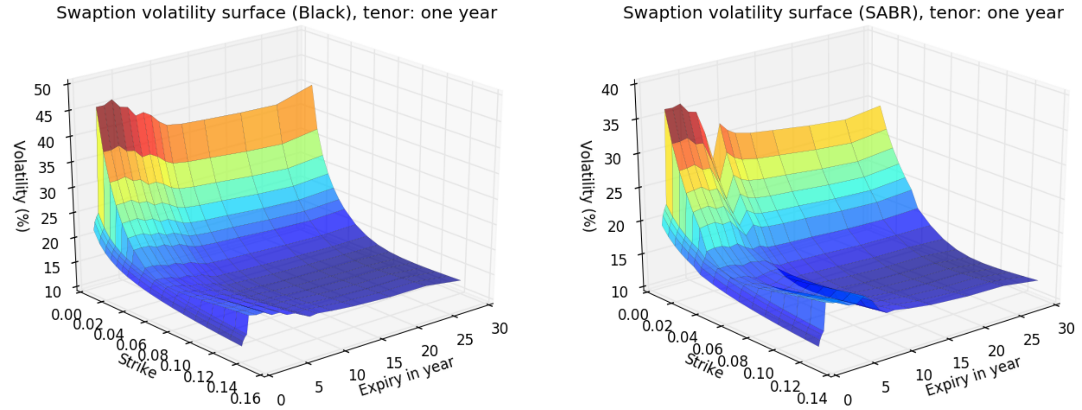

(a) Black implied volatility surface (b) Fitted volatility surface (SABR)

Figure 8: Volatility surface of swaptions with one year tenor

Let us now examine more closely the goodness of fit of SABR model, i.e. the volatility smile. We plot the volatility smile for four different expiry time: one year, 4 years, 7 years, and 30 years. Clearly, as seen in Figure 9a and 9b, the SABR model fits the swaption implied volatility fairly well.

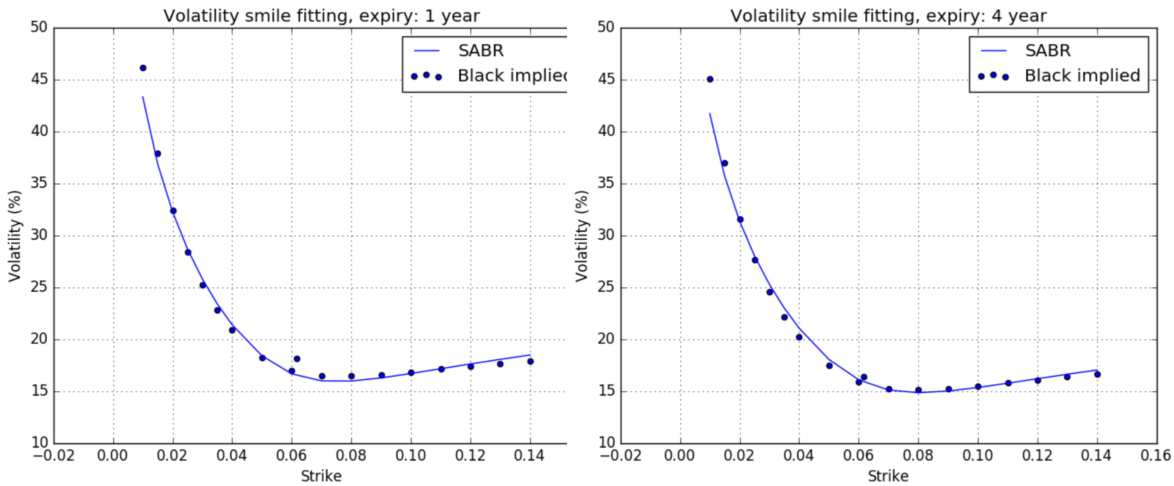

(a) one-year swaption (b) 4-year swaption

Figure 9: Volatility smile for one-year and 4-year swaptions

However, it seems the SABR fitted volatility smile does not quite match with the market implied volatility for the longer expiry time: 7 years and 30 years, especially at lower strike according to Figure 10a and 10b. This result seems to be disappointing at first sight, however the potential explanation is actually reasonably intuitive. Using an analogy in the equity world, the in-the-money call option are generally less traded than at-the-money or out-the-money option thus less liquid.

It is known that the data included in a swaption matrix and corresponding forward rates are not updated at the same frequency, i.e. 'temporal misalignments'. This would cause the inconsistency among the model input thus bad results might be produced.

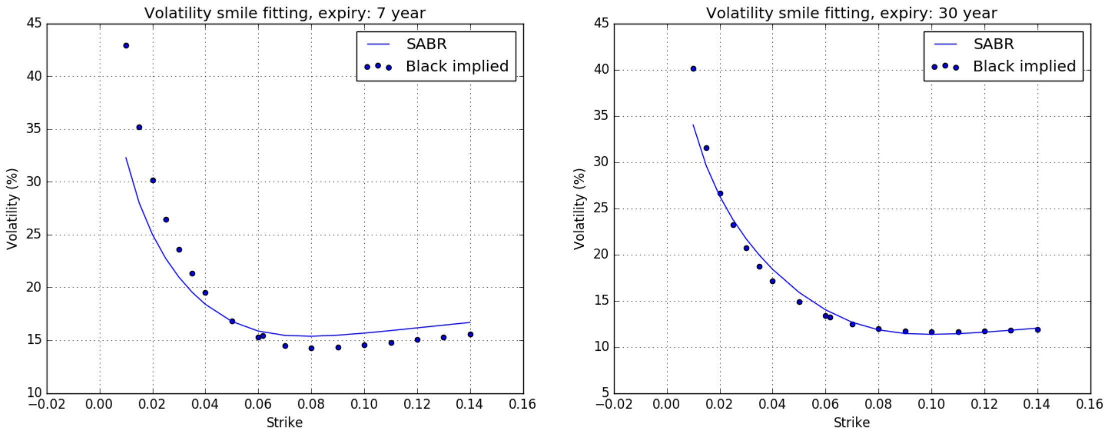

(a) 7-year swaption

(b) 10-year swaption

Figure 10: Volatility smile for 7-year and 30-year swaptions

We have examined empirically the calibration and the performance of the classic SABR model. The main issue raised in our analysis is the high dimension of the model parameters. Volatility smiles are required to be fitted separately, and the output parameter is in three dimension form (in case of fitting swaption volatility cube). Therefore, one can expect the calibration time to be increase exponentially by adding one more strike, expiry or tenor into the current calibration framework.

5.4 Market Case: SABR Extension to LMM

In the literature review, we have seen the SABR extension on Libor market model which address directly the issue of high dimensionality of the SABR model parameters by model the forward rates jointly inspired by the Libor market model under SABR volatility process assumption. The model attempts to capture the dynamics of all forward rates by calibrating two time homogeneous functions, $g(\cdot)$ and $h(\cdot)$, depending on four parameters each for a given tenor. This means the dimension of model parameters to be calibrated is then reduced to two. The calibration algorithm proposed by Rebonato in [2] requires to calibrate the classic SABR model in advance to match The prerequisite of the SABR/LMM model calibration is providing the SABR model has already been calibrated. This implies that the calibration time is actually not being improved by the extension. However, once the model is calibrated, the computation time on swaption prices, especially in the context of evaluation of a large portfolio's position, the model definitely requires much less than the classic SABR model which relies on evaluating swaption price for each expiry, tenor pair separately.

In this section, we shall assess the performance of the SABR/LMM model by fitting separately the classic SABR model and the SABR/LMM model with two caplets with different expiries. We use Monte Carlo simulation to simulate caplets price following the SABR model dynamics. These are then input into Black's model in order to determine the "true" Black implied volatilities which are considered as our benchmark. The pre-fitted classic SABR model parameters value are extracted from [2]. The next step of the comparison is to calibrate the SABR/LMM model parameters using the Black implied volatilities as model input to determine the function $g(\cdot)$ and $h(\cdot)$. The final step is simply plotting the three data sets for both caplets and compare the goodness of fit. In practice, we carried out multiprocessing programming to perform Monte Carlo simulation in parallel to speed up the simulation process.

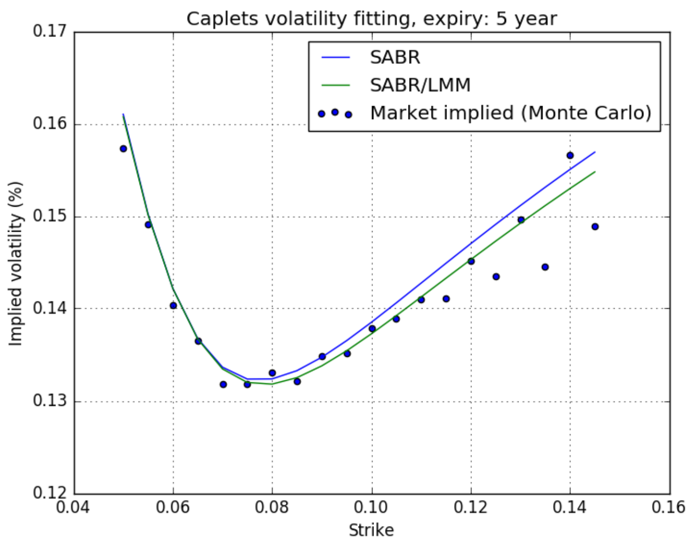

Figure 11: Model fitting for a 5-year caplet. $\alpha = .035, \beta = .5, \rho = -.45, \upsilon = .335, f_0 = .0519$

in Figure 12, we observe that both model fit fairly well the in-the-money 5 year caplets implied volatility. However, both model show bad quality of approximation against a Monte Carlo simulation. Overall, the agreement between the SABR model and the SABR/LMM model can be seen to be relatively good especially for in-the-money caplets.

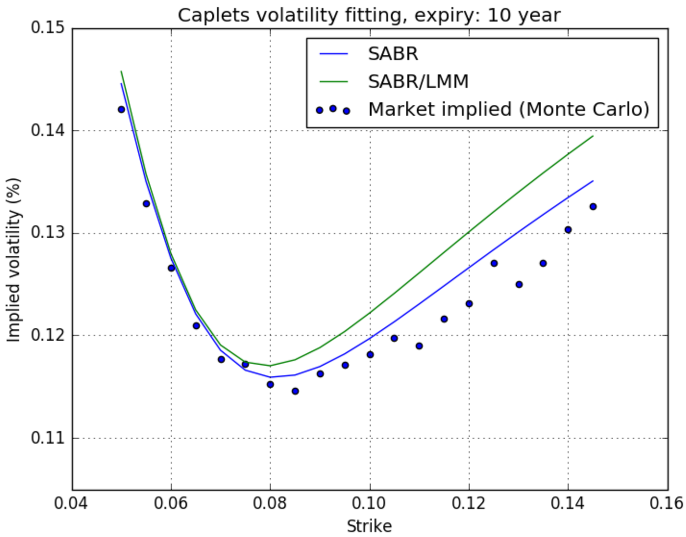

Figure 12: Model fitting for a 10-year caplet. $\alpha = .0305, \beta = .5, \rho = -.395, v = .2825, f_0 = .056$

Similarly, both model fit well the left side of the wing. However the model does not fit quite well the right side of the volatility smile. The result is even Worse comparing to the previous experiment.

We could attribute the imperfectness of the parameters fitting to several root causes. Firstly the simulation scheme we used is the base scheme without adding the high order terms into the simulation path. This could cause the simulation results to be less ideal then expected. Secondly, we did not perform any of the variance control techniques to reduce the simulation variance which also generates discrepancies and oscillation of data points. This would also increase the difficulty of the minimization. Thirdly, the approach of using Monte Carlo simulation on the classic SABR model dynamics to produce the benchmark implied volatilities is somehow bias especially when we compare the results with SABR model itself. Lastly, the assessment of the SABR/LMM model requires more complete empirical tests rather than fitting the simulated implied volatility of two arbitrary caplets.

6 Conclusion

In this thesis, we have introduced the mathematical tools and the market practice on the valuation of vanilla interest rate derivatives such as interest rate swaps, caps and floors, and swaptions. These background knowledges also help reader to realise the key role played by the Black's implied volatility in vanilla interest rate derivatives pricing. We introduced gradually different theories on the implied volatility approximation under the Libor market model, the classic SABR model and the SABR extension of the Libor market model assumptions leveraging on the work of Hagan, Brigo, Rebonato, and their co-workers. These models have been widely studied and implemented. At the end of the literature review, we explained the method used in practice to compute portfolio P&L and sensitivities with respect to the model parameters. It suggests that one can break down the variation of portfolio positions by model parameters in order to assess the model quality. As dived into the technical detail on the calibration procedure of each existing model, we reproduced the problematic revealed in theory, as well in empirical study. For example, the Libor model fail to capture the volatility smile which cannot be neglected in risk management, and the SABR model does not address the correlation between the forward rates. We have also carried out numerical analysis on the SABR/LMM model which attempts to model the joint distribution among the forward rates under the assumption of stochastic volatility. By going through Labordère's approach of the asymptotic analysis on the λ-SABR model implied volatility, we advocate an extension combining the λ-SABR model with the Libor market model for the purpose of improving the existing SABR/LMM model. In this work, we derived the full dynamics of the forward rates under mean-reverting SABR model assumption, proposed a calibration algorithm, and a Monte Carlo simulation scheme to assess numerically the calibration results.

Future work would include the implementation and numerical result on the calibration of the λ-SABR/LMM model, calibration of the SABR/LMM model with latest market caps and swaptions data in order to examine the performance on modelling the joint distribution of the Libor forward rates, and studies of the interest rate derivative sensitivities and hedging strategies in relation to the SABR model.

References

[1] P. Henry-Labordère: A General Asymptotic Implied Volatility for Stochastic Volatility Models, https://arxiv.org/pdf/1102.0998v1.pdf, 2005.

[2] R. Rebonato: A time-homogeneous, SABR-consistent extension of the LMM, https://www.researchgate.net/publication/268337543_A_Time-Homogenous_SABR-Consistent_Extension_of_the_LMM_Calibration_and_Numerical_Results, 2007.

[3] M. S. JOSHI: Achieving Decorrelation and Speed Simultaneously In The Libor Market Model, http://papers.ssrn.com/sol3/papers.cfm?abstract_id=907254, 2006.

[4] I. Fahrner: Differential Geometry, (m, lambda)-SABR and a Formula by Pierre-Henry Labordère, http://papers.ssrn.com/sol3/papers.cfm?abstract_id=1717676, 2009.

[5] R. White, Y. Iwashita: Eight ways to strip your caplets: An introduction to caplet stripping, http://www.opengamma.com/sites/default/files/caplet-stripping-opengamma.pdf, 2014.

[6] C. Homescu. Implied volatility surface: construction methodologies and characteristics, https://arxiv.org/pdf/1107.1834v1.pdf, 2011.

[7] L. B.G. Andersen, V. Piterbarg: Interest Rate Modelling Volume II, 13: 9780984422111 2010,

[8] L. B.G. Andersen, V. Piterbarg: Interest Rate Modelling Volume III, 10: 0984422129, 2010.

[9] D. Brigo, F. Mercurio: Interest Rate Models, Springer Finance, 2006.

[10] P. Hagan, A. Lesniewski: Libor market model with SABR style stochastic volatility, http://www.lesniewski.us/papers/working/SABRLMM.pdf, 2008.

[11] R. Rebonato: Linking caplets and swaptions prices in the LMM–SABR model, https://www.researchgate.net/publication/268174415_Linking_caplets_and_swaptions_prices_in_the_LMM-SABR_model, 2009.

[12] P. S. Hagan, D. Kumar, A. Lesniewski, D. E. Woodward: Managing Smile Risk, http://www.math.ku.dk/~rolf/SABR.pdf, 2002.

[13] D. Brigo, C. Capitani, F. Mercurio: On the joint calibration of the Libor market model to caps and swaptions market volatilities, http://www.cmap.polytechnique.fr/~rama/dea/Brigo-Capitani-Mercurio.pdf, 2001.

[14] J. Pantz: PnL prediction under extreme scenarios, http://papers.ssrn.com/sol3/papers.cfm?abstract_id=2281873, 2013.

[15] A. Estrella: Taylor, Black and Scholes. Series approximations and risk management pitfalls, *Federal bank of New York research paper,* `https://www.newyorkfed.org/medialibrary/media/research/staff_reports/research_papers/9501.pdf`*, 1995.*

[16] R. Rebonato, K McKay, R. White: The SABR/Libor Market Model: Pricing, Calibration and Hedging for Complex Interest-Rate Derivatives, 0470740051, 2009.

[17] T. Alloway: Market Volatility Has Changed Immensely, Bloomberg new article, `http://www.bloomberg.com/news/articles/2015-09-08/market-volatility-has-changed-immensely`*, 2015.*

[18] S. Johnson, B. Nona.: Arbitrage-free construction of the swaption cube. `http://papers.ssrn.com/sol3/papers.cfm?abstract_id=1330869`*, 2009.*

[19] Q. Wu.: Series expansion of the SABR joint density. `http://papers.ssrn.com/sol3/papers.cfm?abstract_id=1367966`*, 2010.*